The Structure and Variability of the Marine Atmosphere around the Santa Barbara Channel

C. E. DORMAN AND C. D. WINANT

Center for Coastal Studies, Scripps Institution of Oceanography, San Diego, California

(Manuscript received 7 August 1998, in final form 10 February 1999)

ABSTRACT

The Santa Barbara Channel is a region characterized by coupled interaction between the lower-level atmosphere, the underlying ocean, and the elevated topography of the coastline. The nature of these interactions and the resulting weather patterns vary between summer and winter.

During summer, synoptic winds are largely controlled by the combined effect of the North Pacific anticyclone and the thermal low located over the southwestern United States, resulting in persistent northwesterly winds. A well-defined marine atmospheric boundary layer (MABL) with properties distinct from the free atmosphere above is a conspicuous feature during the summer. The wind has different characteristics in each of three zones. Maximum winds occur in the area extending south and east from Pt. Conception (zone 1), where they initially increase as they turn to follow the coast, then decrease farther east. Winds are usually weak in zone 2, located in the easternmost part of the channel, offshore from the Oxnard plain. Winds are also weak in zone 3, sometimes reversing to easterly at night, in a narrow band located along the mainland coast. Summer air temperature at the surface follows the SST closely and varies significantly with location. Summer sea level pressure gradients are large, with the lowest pressure occurring on the northeast end of the Santa Barbara Channel. Diurnal variations are strongest in summer, although the modulation is weakest in zone 1. The diurnal variation is parallel to the coast in all of zone 3 but the Oxnard plain, where it is perpendicular to the coast. The height of the marine layer varies between 300 m in late afternoon and 350 m in late morning.

In winter, synoptic conditions are driven by traveling cyclones and sometimes accompanied by fronts. These are usually preceded by strong southeast winds and followed by strong northwest winds. Atmospheric parameters are distributed more uniformly than in summer, and diurnal variations are greatly reduced. Sea level air temperature and pressure are more spatially uniform than in the summer.

Spatial variations in the observed fields in the summer are consistent with a hydraulic model of the MABL as a transcritical expansion fan. The summertime situation is governed by a coupled interaction between the atmosphere and the underlying water. The ocean influences the density of the MABL to the extent that it behaves distinctly from the free atmosphere above, resulting in strong winds polarized in the direction parallel to the coast. In turn, these winds provoke an upwelling response in the coastal ocean, which in part determines the surface properties of the water.

1. Introduction

The earliest account of the meteorological conditions in the Southern California Bight was made by Dana (1841), who described the strong southerly winds that could precede a frontal passage and were responsible for the grounding of ships against the lee shore of Santa Barbara. Ship-based climatology (Nelson 1977) reinforces the modern perception of coastal winds along the west coast of the United States: these winds are believed to be strong along the north coast and weak off southern California. Even more recent analysis of West Coast automated buoy winds revealed that there are two summer mean monthly wind speed maxima: one along northern California just north of San Francisco and the other at the western mouth of the Santa Barbara Channel (Dorman and Winant 1995).

Reports from automated buoys and ships show that the general open coast winds approaching Pt. Conception are from the northwest and stronger in the summer (Nelson and Husby 1983; Dorman and Winant 1995). Based upon land stations and experience, DeMarrias et al. (1965) suggested the afternoon sea surface winds sweep around Pt. Conception and along the Santa Barbara Channel, exiting mostly over the Oxnard plain or to the southeast toward Los Angeles (Fig. 1). In contrast, sea surface winds in the early morning along the north and east portions of the Santa Barbara Channel are light and variable. Wind direction along the coast and valleys is reversed so as to be from the land direction during weak, early morning, winter drainage winds. Aircraft

Corresponding author address: Clive E. Dorman, Center for Coastal Studies, Scripps Institute for Oceanography, San Diego, CA 92093-0209.

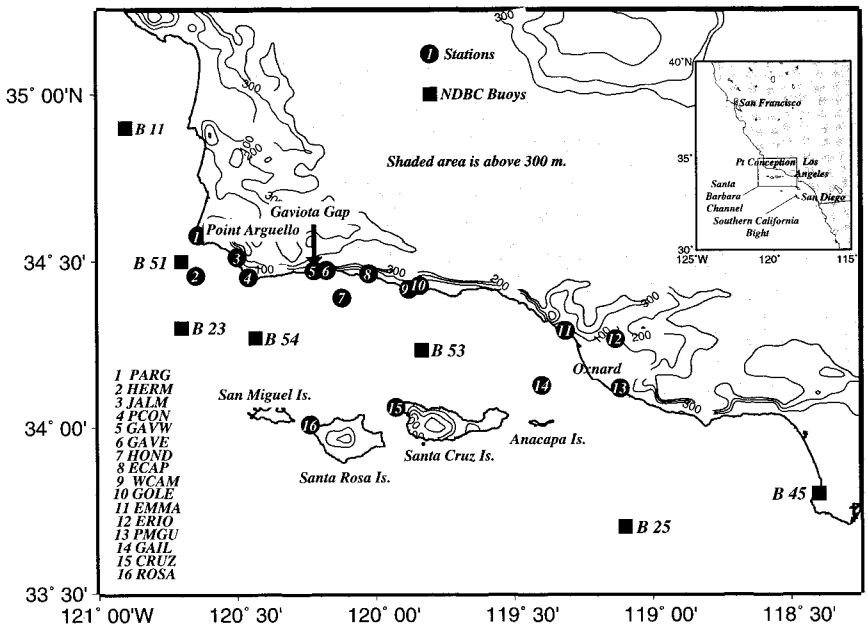

FIG. 1. Station locations and topography.

and buoy measurements show the acceleration of the sea surface winds around Pt. Conception into a maximum at the center of the western mouth of the Santa Barbara Channel (Brink and Muench 1986; Caldwell et al. 1986). Buoy, coastal stations, and finer-scale analysis of ship winds confirm that winds in the southerly and inner waters of the Southern California Bight are generally weak and westerly (Dorman 1982; Halliwell and Allen 1987; Dorman and Winant 1995).

During the extended summer, the area is dominated by a persistent, low, subsidence air temperature inversion caused by the northeastern Pacific anticyclone. Based upon limited observations, Neiburger et al. (1961) suggested that the inversion base over this area of the coast is around 400-m elevation, and the strength of the inversion is 10°C. The capped layer below is referred to as the Marine Atmospheric Boundary Layer (MABL). Aircraft observations in August–September 1966 showed that the inversion base was lowest at Gaviota (240 m), less that 350 m in the Santa Barbara Channel, and higher away from it, especially toward Los Angeles (Edinger and Wurtele 1972). The depth of the marine layer at the coast can vary from 0 to 800 m (e.g., Edinger 1959, 1963; Baynton et al. 1965; Dorman 1985a; Wakimoto 1987).

The South Central Coast Cooperative Aerometric Monitoring Program (SCCCAMP) took place for 5 weeks in September and October 1985 (Dabberdt and Viezee 1987) to monitor air pollution events. A review of background measurements and four intensive measurement periods points out synoptic and mesoscale patterns associated with high ozone. These patterns include a cyclonic eddy centered in the Santa Barbara Channel and an eddy at Gaviota (Douglas and Kessler 1991; Hanna et al. 1991). A numerical study by Kessler and Douglas (1991) found that a combination of steep topography and diurnal heating with cross-ridge flow results in trapping and westward phase progression of wind direction shifts along the south slopes of the mountain behind Santa Barbara.

Certain synoptic situations force locally distinct responses. Santa Anas are gusty, offshore, warm, dry winds that occur from autumn to spring when high pressure is situated over the Great Basin of Nevada and Utah (Sommers 1978). Santa Anas are usually strong at the mouths of river valleys. The reach of the offshore surface winds is believed to be limited but may extend to the distant islands in extreme cases (DeMarrias et al. 1965).

A cyclonic eddy within the marine layer covering the Southern California Bight may occur at any time of the year and is usually associated with an elevated air temperature inversion base and a stratus overcast (e.g., Rosenthal 1968, 1972; Bosart 1983; Dorman 1985a; Wakimoto 1987; Mass and Albright 1989; Clark and Dembek 1991). It has been a local custom to refer to all such features as ''Catalina eddies,'' but different events may be associated with different causes and dynamics.

The interaction of synoptic-scale features with the topography and the stable marine layer may result in topographically trapped events. At the very least, this interaction contributes significantly to the topographic trapping of the dynamics of the response. There has been considerable discussion about whether there might be solitary Kelvin waves or gravity currents present (e.g., Dorman 1985a, 1987; Mass and Albright 1987; Wakimoto 1987; Clark and Dembek 1991; Eddington 1985; Eddington et al. 1992; Reason and Steyn 1992). There

TABLE 1. Stations.

Designator	Station	Lat N	Lon W	Elev (m)	Variables	Operator
B11	Buoy 46011	34°54′	120°54′	0	W, T_a, T_s, P	1
B23	Buoy 46023	34°18′	120°42′	0	W, T_a, T_s, P	1
B25	Buoy 46025	33°42′	119°06′	0	W, T_a, T_s, P	1
B45	Buoy 46045	33°48′	118°24′	0	W, T_a, T_s, P	1
B51	Buoy 46051	34°30′	119°42′	0	W, T_a, T_s, P	1
B53	Buoy 46053	34°14′	119°50′	0	W, T_a, T_s, P	1
B54	Buoy 46054	34°16′	119°26′	0	W, T_a, T_s, P	1
CRUZ	Santa Cruz Island	34°04′	119°56′	20	W, T_a, P	2
ECAP	El Capitan	34°28′	120°01′	39	W, T_a	3
EMMA	Emma Woods Beach	34°17′	119°19′	3	W, T_a	4
ERIO	El Rio	34°16′	119°08′	34	W, T_a	4
GAIL	Gail Platform	34°08′	119°24′	30*	W, T_a, P	2
GAVE	Gaviota East	34°28′	120°11′	34	W, T_a	3
GAVW	Gaviota West	34°28′	120°13′	29	W, T_a	3
GOLE	Goleta	34°26′	119°50′	3	W, T_a, RP	5
HOND	Hondo Platform	34°23′	120°07′	44*	W, T_a, P	2
JALM	Jalama Beach	34°31′	120°30′	6	W, T_a	3
HERM	Hermosa Platform	34°27′	120°39′	40*	W, T_a, P	2
PARG	Pt. Arguello	34°35′	120°38′	52	W, T_a, P	1**
PCON	Pt. Conception	34°27′	120°27′	55	W, T_a	3
PMGU	Pt. Mugu NAS	34°07′	119°07′	4	W, T_a, P	6
ROSA	Santa Rosa Island	34°00′	120°14′	17	W, T_a, P	2
WCAM	West Campus	34°25′	119°53′	9	W, T_a	3

W = winds, T_a = temp air, T_s = temp sea, P = pressure, RP = radar profiler.
* = anemometer height.
** = CMAN station.
1 = National Data Buoy Center.
2 = Scripps Institution of Oceanography.
3 = Santa Barbara Air Pollution Control District.
4 = Ventura Air Pollution Control District.
5 = NOAA, ETL, Boulder.
6 = U.S. Navy.

has also been the suggestion that part of the formation phase of some Catalina eddies might involve trapping.

The Center for Coastal Studies at Scripps Institution of Oceanography has been involved in a multiyear oceanographic program on the Santa Barbara Channel sponsored by the Minerals Management Service. Part of this program included making automated surface measurements and retrieving other measurements obtained by air pollution control districts. The result is an extensive network of surface stations (Fig. 1) with limited upper-air measurements. The object of this paper is to describe the atmospheric conditions in and around the Santa Barbara Channel and to examine the possible underlying dynamics.

2. Observations

The Santa Barbara channel is approximately 40 km wide and 100 km long (Fig. 1). The coastline at Pt. Conception near the northwestern edge of the channel is sharply curved, directed meridionally north of Pt. Arguello and zonally to the east of Pt. Conception. The north side and east end of the Santa Barbara Channel is lined with topography that extends abruptly to well above 300 m. On the east end, the low Oxnard plain forms the mouth of a river valley that extends upward and to the northeast. Lining the south side are the four Channel Islands: San Miguel, Santa Rosa, Santa Cruz, and Anacapa. The center two islands extend above 400 m. Gaps exist between the islands, which can act as wind funnels. Surface air exiting the southeast end of the channel may continue to the greater Los Angeles basin, to the southeast.

There are 21 automated surface meteorological observation networks used for this analysis. Scripps Institution of Oceanography (SIO) maintained three automated stations on oil platforms and two on islands (Fig. 1, Table 1). The National Data Buoy Center (NDBC) made hourly observations from six buoys and one coastal station (Hamilton 1980). Hourly coastal automated observations were also available from six Santa Barbara Air Pollution Control District stations and two Ventura Air Pollution Control District stations. Finally, hourly data was provided by the U.S. Navy at Pt. Mugu. The SIO and air pollution control stations data are averaged over the hour. The NDBC and Pt. Mugu stations are an average of several minutes near the hour. Winds and air temperature were measured at all stations. Pressure was recorded for the SIO and NDBC stations and Pt. Mugu. Sea temperatures were taken only at the NDBC buoys.

The atmospheric pressure at all stations was adjusted

to sea level as described by Dorman and Winant (1995). Buoy winds were adjusted to 10 m above sea level following the method described by Large and Pond (1981) for a neutral atmosphere. Winds from oil platforms were not adjusted owing to the uncertainty of the effect of the platform structure on the wind field, which can be positive or negative (Thornthwaite et al. 1965). HERM (see Table 1 for station name definitions) wind observation at 40-m elevation is similar in magnitude to the nearby NDBC buoy 51 (B51) wind observation at 10 m. No adjustments were made to the coastal or island station winds.

Vertical profiles are from three different instruments. The National Oceanic and Atmospheric Administration Environmental Research Laboratory (Boulder, Colorado) maintained a radar profiler at Goleta from May to September 1996. This station is on a low coastal plane on the north side of the Santa Barbara airport, 2 km from the ocean. The radar profiler provided hourly vertical profiles of horizontal winds at 100 m vertical spacing. Hourly, consensus-averaged winds, which are used here, were calculated from measurements made every few minutes with some limited intervals of interference from birds removed. Vertical profiles of a virtual temperature, assumed to be the air temperature, were constructed from a radio acoustic sounding system that is operated in conjunction with the radar profiler. Details about the radar profiler, radio acoustic sounding system, and averaging techniques are described by Ralph et al. (1998).

A U.S. Navy–sponsored Variability of Coastal Atmospheric Refractivity (VOCAR) field program operated eight land-based, upper-air sounding stations over the Southern California Bight from 23 August to 3 September 1993 (Paulus 1995). One of these was a tethered balloon station at Gaviota on the low, narrow coastal plain at 60-m elevation and 600 m from the ocean. Here, 2-hourly tethered balloon soundings were made for a 3-week period ending on 3 September 1993. Surface data variations during VOCAR are described in Fisk (1994).

3. Overview

Averages based upon multiyear analysis of buoy winds over southern California coastal waters suggest that May–July and December–February are representative of summer and winter while the other months are transitional (Dorman and Winant 1995)—a scheme that we adopted for this paper. A 2-yr time series for two stations for December 1995–November 1996 is shown in Fig. 2 to give an overview of the annual and synoptic-scale variability. The plotted winds are rotated into components along and across the direction of maximum variance based upon a year's observations (the principal axis or PA). Buoy 54 is typical of the faster wind speed stations in the western mouth. It has more direction reversals in the winter than in the summer due to the stronger synoptic events in the winter. Summer winds are more persistently from a northerly direction but still have large variations in magnitude. Other overwater stations have similar annual structure but synoptic-scale variations of lesser magnitudes.

The north coastal stations generally have weak winds, and those in the western half are punctuated by spikes in the wind speed. Typical of this group is ECAP, which has dominantly weak, along-coast variations with little seasonal trend. Cross-coast, reversing wind pulses of short duration occur mostly in the winter. Offshore-only pulses happen mostly between March and June.

The scalar variables of pressure, air temperature, and sea surface temperature (SST) are shown only for B54, which is representative of the other stations. Maximum pressure variability is associated with winter synoptic-scale variations. Minimum pressure and variability are in the late summer when synoptic variations are greatly weakened and the large-scale North Pacific anticyclone retreats to its most northern position. Sea temperature is a weak minimum in the early summer to midsummer, reflecting the dominance of wind-driven, coastal upwelling. The air temperature is held close to that of the sea as a persistent, dense atmospheric marine boundary layer is present. The marine layer is isolated from exchange with air above by an air temperature inversion and from horizontal exchanges with inland extremes by topography. The layer's dominant thermal contact is via long trajectories over the sea, which has a large heat capacity. The result is that the mean monthly sea minus air temperature at B54 (not shown) has a difference of -0.6°C in April and a maximum of 1.3°C in September.

A distinct annual trend is seen in the monthly mean wind vectors at the western end of the Santa Barbara Channel and Pt. Conception area (Fig. 3). The strongest speeds are in the summer (maximum is April and May 1996) and weakest in the winter (minimum is February 1996) but always from a northwesterly direction. The annual trend has similar annual phase but much weaker magnitude in the eastern end of the channel. Stations on the north channel coast and east of Pt. Conception, with the exception of Ventura (EMMA), have weak means with no significant annual speed trend that is typified by GAVE and WCAM.

The remainder of this paper is organized around examining the two representative seasons. The summer structure and variations are presented first. This is followed by a description of the winter structure. Next is a section on the offshore winds at Gaviota and eddies in the wind field. This is followed by a discussion of dynamics based on the earlier portions of this paper.

4. Summer structure and variations

a. Mean fields

Maps of the mean wind and principal axes (PA) direction and strength are shown in Fig. 4 for May–July

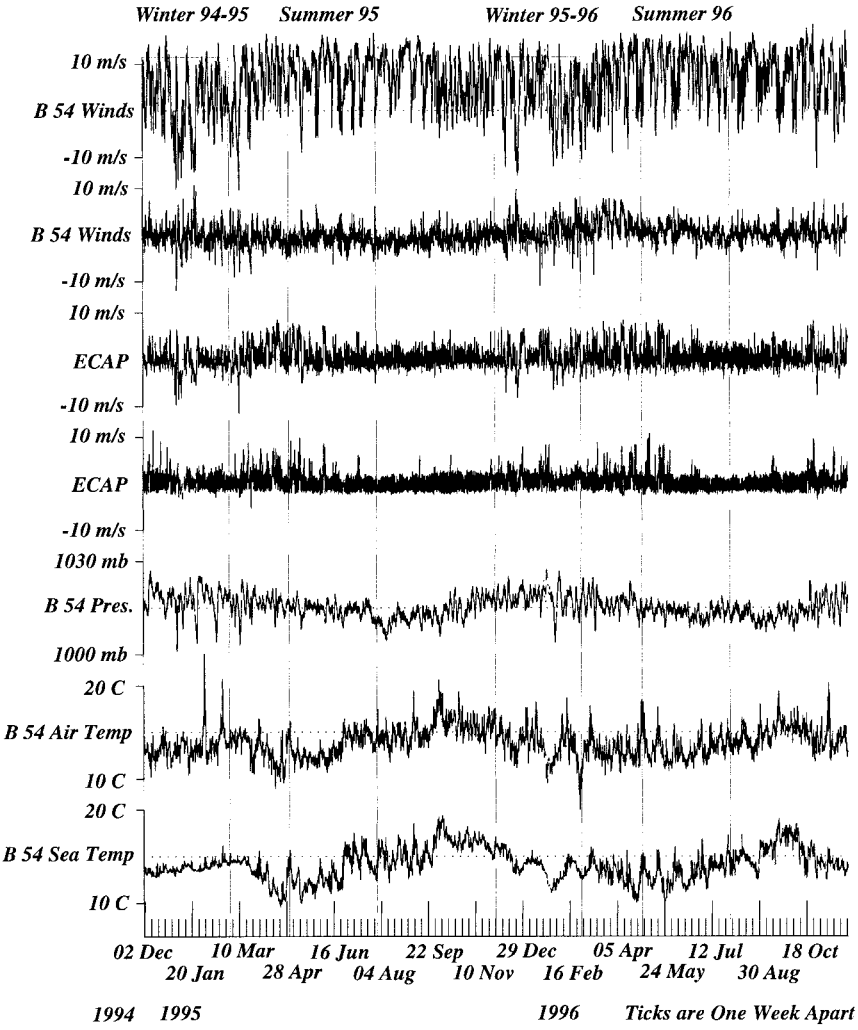

FIG. 2. Winds along and across the principal axes for B54 and ECAP. Pressure, air temperature, and sea temperature is for B54. The top frame is the B54 major axis of the wind (along 306°T), the second frame is the B54 minor axis (along 216°T), the third frame is ECAP winds along the major axis (along 311°T), and the fourth frame is ECAP winds along the minor axis (along 221°T).

1996 (values in Table 2). B23 and JALM were not available for this period, so averages for May–July 1995 have been substituted.

The sea level winds approach the channel from the northwest, accelerate, and turn cyclonically around Pt. Arguello, reaching a maximum in the middle of the western channel (Fig. 4). Once past this point, the near-surface air slows as it continues down the center of the channel, exiting to the east into the Ventura Valley or continuing over water to the southeast toward the greater Los Angeles Valley. Compared to the center channel, winds are weaker at the islands on the south edge and very weak along the northern coast east of Pt. Conception. Standard deviations are less than the means for the overwater stations in the western mouth but much larger than the weak means along the north side, which are east of Pt. Conception and the overwater stations on the east end.

The Santa Barbara Channel stations may be divided into three zones according to the character of the wind variations. Station B54 is typical of zone 1, where stations have a high velocity and strong polarization with winds dominantly from a north-northwest direction (Fig. 5). At B54 during the summer of 1996, 84% of the days had winds greater than 10 m s^{-1} for part of the day, 67% of the days had winds from 306° (also along the PA) greater than 5 m s^{-1} for the entire day, 16% had winds in the same direction but between 0 and 5 m s^{-1}, while 19% had winds from 126° for part of the day.

At B53, 22% of the days had winds from the west along the PA greater than 10 m s^{-1} during part of the day, 34% of the days had winds that were from 80°

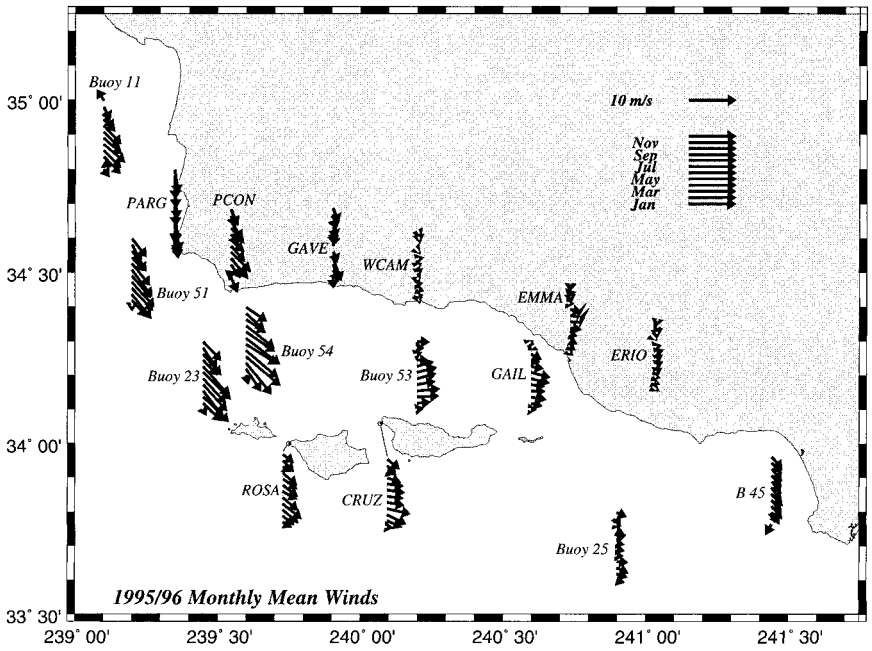

FIG. 3. Wind vector mean monthly annual trend. Monthly mean winds for Jan (lowest arrow) through Dec 1996 (uppermost arrow). Speeds are greatest in the western channel mouth in the summer.

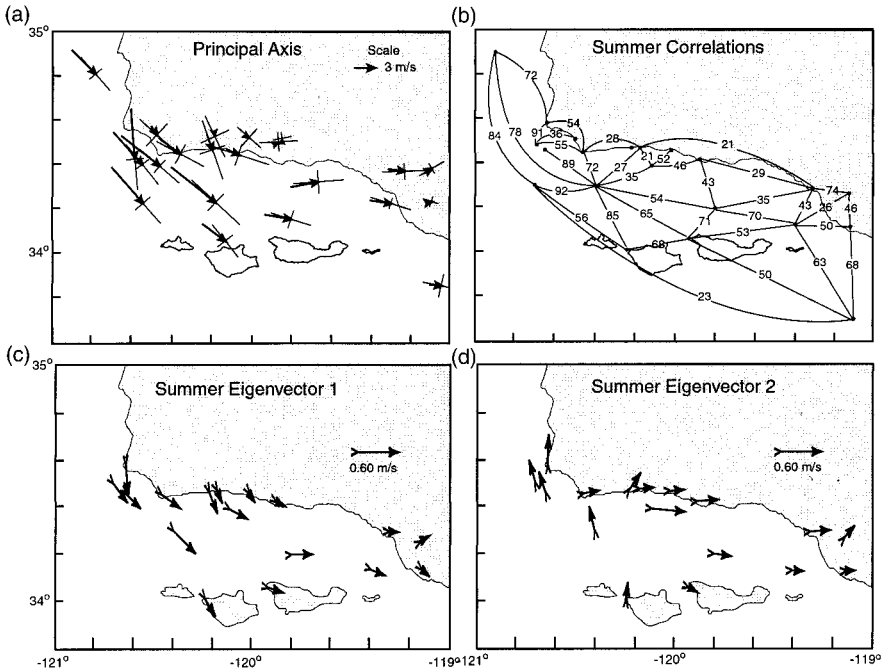

FIG. 4. (a) Summer mean surface wind speed and principle axes (PA). The arrow that flies with the wind represents the mean. The cross at the end of the wind vector is the wind standard deviation with the long side the maximum magnitude and orientation and the short side the minimum. (b) Summer wind correlations along station PAs. (c) and (d) First and second empirical orthogonal functions for the summer.

TABLE 2. Station wind characteristics.

Station	Mean speed (m s^{-1})	Mean direction (deg)	PA direction (deg)	Major axis speed (m s^{-1})	Minor axis speed (m s^{-1})	Speed difference (m s^{-1}; 16–08 PST)
			Summer			
B11	5.2	136	139	3.4	1.2	1.4
B23	7.3	139	138	4.1	1.5	0.7
B25	1.8	96	101	2.9	1.8	2.9
B45	2.5	138	120	2.0	1.8	2.3
B51	6.6	138	142	3.9	1.2	0.0
B53	4.3	80	86	3.8	1.8	3.4
B54	8.7	128	133	5.0	1.7	1.8
Cruz	4.1	84	92	3.2	1.4	2.2
ECAP	0.5	120	131	2.4	1.8	1.1
EMMA	2.5	97	88	3.4	1.3	4.1
ERIO	1.4	60	59	2.2	0.9	3.2
GAIL	3.2	98	107	3.2	0.9	2.8
GAVE	0.4	173	155	3.4	2.3	1.1
GAVW	2.6	160	161	4.8	2.0	1.5
HERM	7.5	129	131	3.9	1.3	1.0
HOND	2.0	114	108	4.9	1.8	4.6
JALM	1.6	145	133	3.5	2.4	2.7
PARG	7.8	176	175	4.7	1.4	1.3
PCON	4.1	127	119	4.0	1.7	4.5
PMGU	0.9	81	107	1.1	0.8	1.8
ROSA	4.3	111	126	3.2	1.5	1.3
WCAM	0.7	63	86	2.9	1.5	1.5
			Winter			
B11	0.8	153	142	5.9	2.4	0.8
B23	4.3	142	131	6.4	2.5	0.7
B25	1.8	120	103	4.3	2.6	0.5
B45	1.6	140	108	3.2	2.5	0.9
B51	3.5	149	132	6.6	2.2	0.4
B53	1.9	89	98	5.3	2.1	1.4
B54	4.2	134	123	6.8	2.6	0.7
CRUZ	2.4	111	107	5.0	2.6	1.4
ECAP	1.1	175	116	2.7	1.7	0.7
EMMA	1.2	179	85	3.6	1.7	0.5
ERIO	0.9	191	63	2.7	1.5	0.0
GAIL	1.3	93	115	4.6	1.7	1.6
GAVE	1.2	188	125	3.5	2.1	0.7
GAVW	3.0	167	140	4.2	2.1	2.7
HERM	3.3	136	129	6.2	1.9	1.4
HOND	1.6	142	112	5.4	2.0	2.0
JALM	1.7	71	105	2.9	2.1	2.3
PARG	3.6	175	165	6.7	2.1	0.4
PCON	2.3	155	119	5.0	1.9	0.9
PMGU	0.1	118	108	1.3	0.9	0.4
ROSA	2.9	114	112	4.0	2.1	1.1
WCAM	0.7	158	95	2.8	1.7	0.6

greater than 1 m s^{-1} for part of the day. On only 8% of the days did B53 have any winds from 260° greater than B54 had from 306°. Other stations in this zone are the northern mouth stations of Pt. Arguello, Hermosa, B51, Pt. Conception, and the island stations of SROS and SCRZ.

Zone 2 is in the eastern end of the channel, adjacent to the Oxnard plain. This zone has the single station of GAIL, which has two different major wind alignments (Fig. 5). The dominant daily winds were from 280°, which occurred 74% of the summer days, while the winds greater than 1 m s^{-1} for at least 3 h from 135° occurred on 25% of the summer days. However, only 1 day had afternoon winds from 135° for greater than 3 h. As will be discussed later, this does not support the dominance of a midchannel eddy. On 23% of the summer days, both GAIL and B53 had a component from the east-southeast in excess of 1 m s^{-1}.

Zone 3 stations are along the north and east coast. They have a diurnally reversing wind direction. For the stations from GAVE to EMMA, the dominant wind alignment along the coast is generally from the west in the afternoon and the east in the night and early morning. GAVE winds are mostly parallel to the coast, with some scatter from the northwest that exceeds 10 m s^{-1} (Fig. 5). HOND, just 6 km offshore, has stronger along-

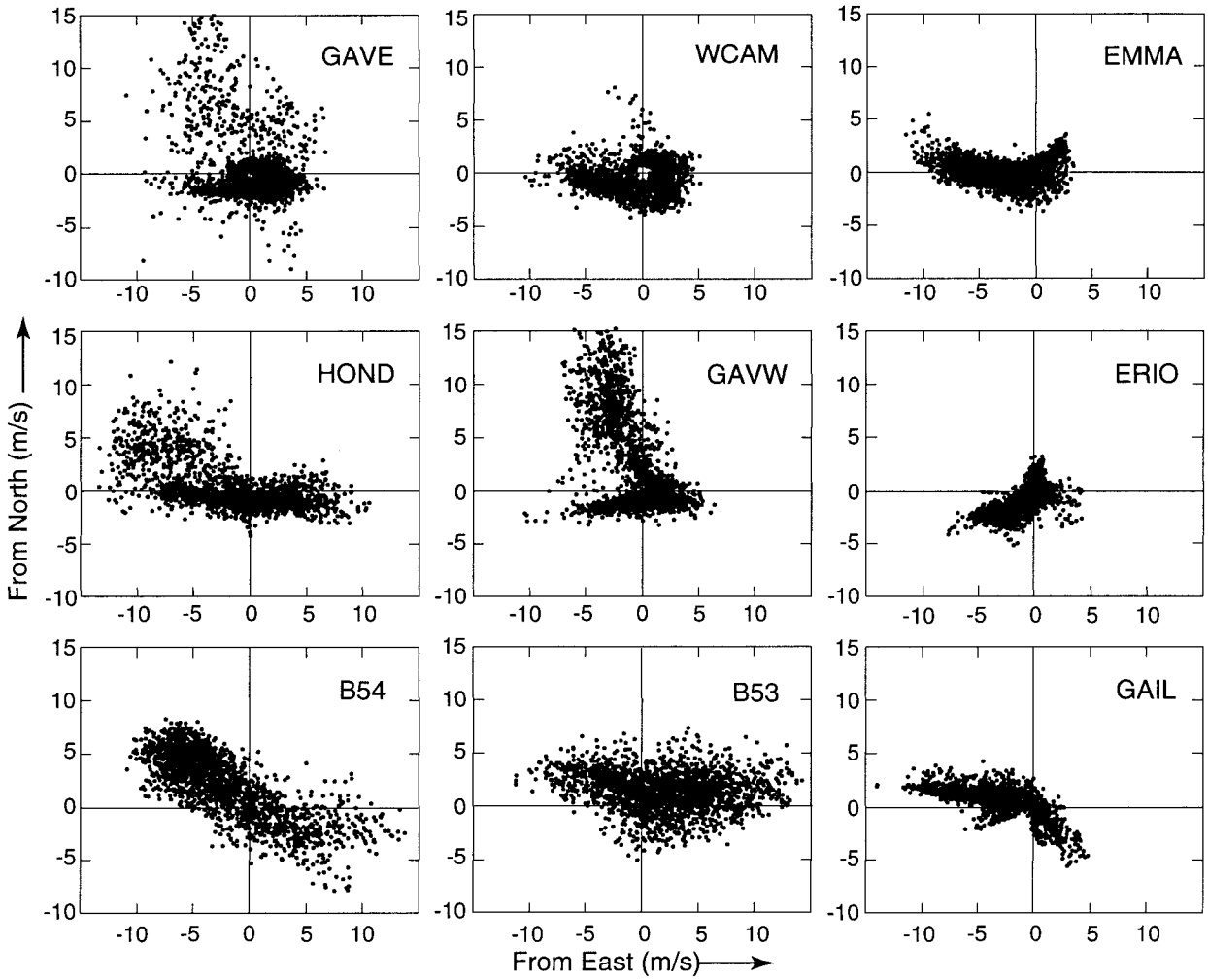

FIG. 5. Scatterplots of summer winds at representative stations. All summer wind hourly observations for a station are plotted relative to true north. Fastest mean winds and greatest polarization is at B54.

shore winds from either direction than GAVE or GAVW. WCAM has weaker alongcoast winds that are a little stronger from the west but lack the minority cases of strong offshore component experienced by the more western coastal stations. EMMA has no strong offshore component, but the westerly component is faster than the easterly component. ECAP and JALM are similar to GAVE (not shown). GAVW has two dominant modes: one is the alongshore, diurnally reversing mode and the other GAVW mode is a strongly polarized, high speed, offshore wind.

ERIO, on the Oxnard plane, experiences a diurnally reversing, cross-coast sea/land breeze as air moves up or down the Ventura River valley. The weak, semidiurnal speed maximums are in 2–4 m s^{-1} range and are generally unrelated to the dramatic speed changes in the western mouth such as at B54. Not included in zone 3 are PARG and PCON, which are on low points of land that extend out beyond the narrow coastal plane and have wind characteristics of zone 1 (stronger winds polarized from the north or northwest and not diurnally reversing along coast).

There is a distinct asymmetry with lower pressure on the north side (Fig. 6), in the cross-channel pressure field for the mean summer sea level pressure. The pressure field is lowest in the eastern end of the channel and even lower toward Los Angeles (not shown). There is a small pressure maximum around Pt. Arguello that may be associated with a thickened marine layer and increased clouds.

b. Correlations and EOFs

Correlations for the summer season were computed among the stations for the wind along the PA (Fig. 4). The best correlations (0.7–0.9) are between the zone 1 stations in the western mouth of the channel (B54 with others). Weak correlations (0.5–0.6) are between the western mouth (as represented by B54) and the eastern central stations as B53 and CRUZ. Poor correlations

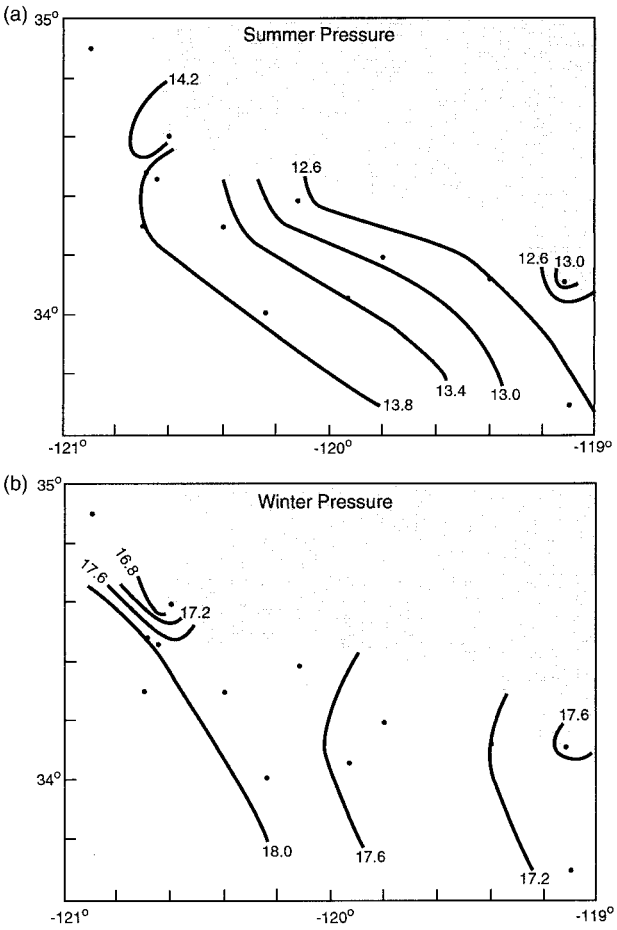

FIG. 6. (a) Summer and (b) winter mean sea level pressures (hPa). A cross-channel gradient occurs only in the summer.

exist between the center line channel stations (B54, B53) and the land coastal stations (GODW to EMMA and HOND). Even though it is over water, HOND is poorly related to B54 as well as the coastal stations. In contrast, the two stations on exposed points (PARG and PCON) are moderately correlated with the near, overwater stations (B54, HERM).

The covariability of the horizontal structure of the surface wind field was examined by EOF analysis (Lorenz 1956). A separate analysis (Fig. 4) was done for the summer (May–July 1996) and winter (December 1995–February 1996). The weight of the first three modes of each season are significantly different (Table 3). The eigenvector patterns are similar for the summer and winter. Eigenvector 1 is all in an east–west direction, with the largest values in the western mouth. This mode is associated with the dominant, synoptic-scale variations seen in both the summer and the winter.

Eigenvector 2 is oriented north–south in the western mouth and east–west in the eastern half. This mode is associated with diurnal variations that are also important in all seasons. This is a formal confirmation of an earlier noted observation: the majority of the land stations

TABLE 3. Eigenvector weights.

Summer EOF		Winter EOF	
Mode	Weight	Mode	Weight
1	0.44	1	0.65
2	0.18	2	0.09
3	0.10	3	0.44

(zone 3) scatterplot winds are along coast. On the other hand, the western mouth stations (SROSA, B54, B51/HERM, and PARG) are at right angles to the eastern half and the coastal land stations in the channel. The effect is that the eastern station component is from the west while the western is from the south, creating a zone of divergence between the two. If both sets of stations are reversed, there will be a zone of convergence between the two.

The strongest and most significant values for eigenvector 3 (not shown) are for the central, north-coast stations that have a strong, cross-shore, northerly component. This is associated with the lee events and cross-coast wind events that are mostly seen at GAVW, GAVE, and HOND.

Time series of the first two EOF modes are shown in Fig. 7 for summer and winter. The first mode is dominated by synoptic-scale variations of the order of 10 days' duration. The second mode is dominated by diurnal variations. The variation of both time series is similar in magnitude and period for the summer and winter seasons.

c. Synoptic variability

The most frequently occurring summer event is high speed, sustained winds from the northwest followed by a short period of weak winds. Fastest winds are at the western mouth of the Santa Barbara Channel and are associated with strengthened along-coast sea level pressure gradient and weak cyclonic circulation in the mid-level of the atmosphere. A typical case is shown for the period 2–10 July 1996. The main sea level synoptic features are the North Pacific anticyclone to the northwest (to the northwest of the area shown in Fig. 8) with a heat low in the southwest United States. North of Pt. Conception, the along-coast pressure gradient strengthens from 3 to 5 July then decreases again on 9 July as the heat low expands. Sea level pressure gradients over water are consistently weak southeast of Pt. Conception for the entire period despite the variation in sea level speeds at the western mouth (Fig. 9). At 700 hPa (not shown) an approaching trough on 3 July weakens as it moves over the California coast on 7 July and to eastern California on 9 July.

The sea level winds in zone 1 respond to synoptic variations. Examples of selected stations are shown in Fig. 9 (the wind direction has been rotated to the station's PA so as to make viewing easier). After a brief

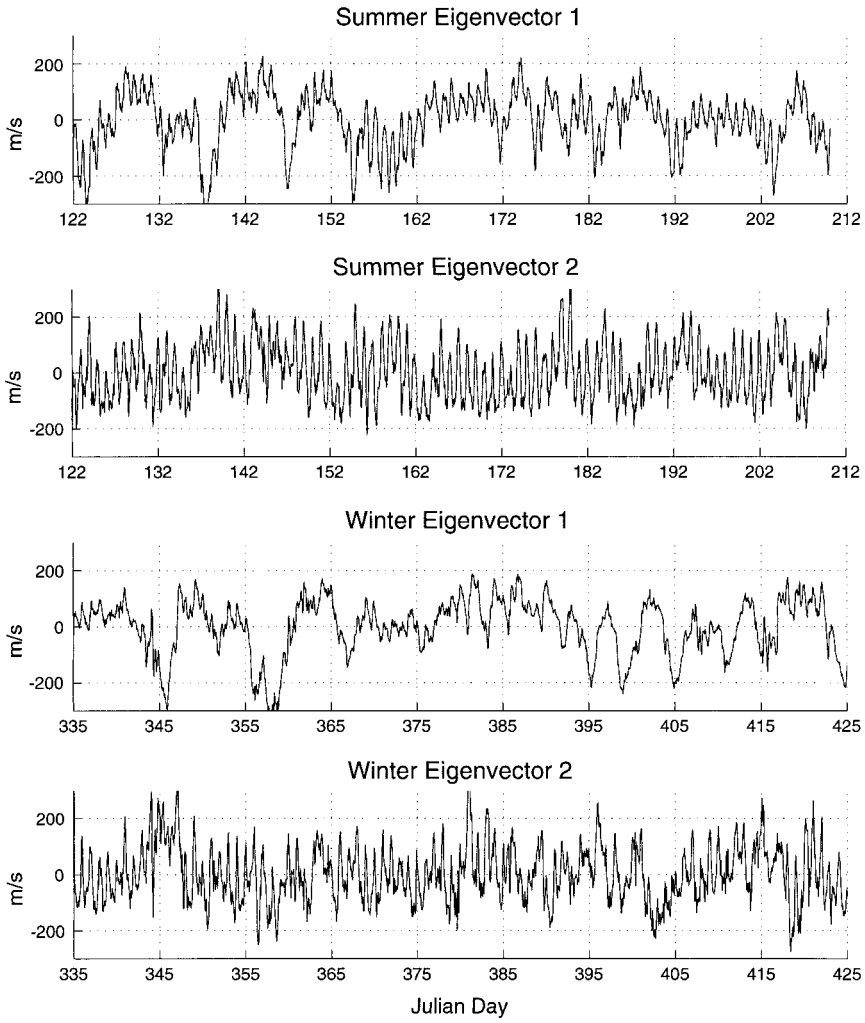

FIG. 7. Time series of the first and second eigenvector modes of the winds for the summer and the winter. The synoptic scale dominates the first mode and the diurnal scale is predominant in the second.

period of weak winds, strong inbound northerly winds persisted at B51 for 7 days with stronger winds at B54. Once past B54, wind speeds decrease to B53, then to GAIL (not shown), to reach a minimum speed at ERIO in the eastern end. Indeed, it would be hard to determine the state of the winds at the western mouth of the SB channel if only the El Rio observations were available. Winds at the channel islands (SROS and SCRZ, not shown) are somewhat weaker but correlated with the buoy winds at B54 and B51. The winds over the zone 3 land stations were generally west–east with only an occasional clear, cross-coast, northerly velocity such as occurred at GAVE (and GAVW and HOND) for 4 h early on 5 July. While it is the local custom to call such offshore events ''sundowners'' (Ryan 1996), the wind was observed only in the immediate area of GAVW, which is at the foot of the ridge height minimum of the Santa Ynez mountains. The next event was weak winds and reversals on 9–10 July, becoming the second most frequently occurring event over the open channel.

d. Diurnal variability

Generally, all winds are strongest in the early afternoon and weakest around sunrise. The zone 3 coastal land stations in Fig. 4 have weak, along-coast winds that are diurnally reversing. The exceptions are ERIO and PMGU, where the winds are cross-shore. The strongest wind reversals are at the land stations of HOND and EMMA. The eastward flow decreases and diurnal range increases from B54, to B53, to GAIL, to ERIO. The diurnal character is substantially different for the easternmost station on the Oxnard plane, which has a maximum between 1100 and 1600 PST and reverses direction to weakly offshore at night (2100–0700 PST).

Summer temperatures are for the May–July 1996 pe-

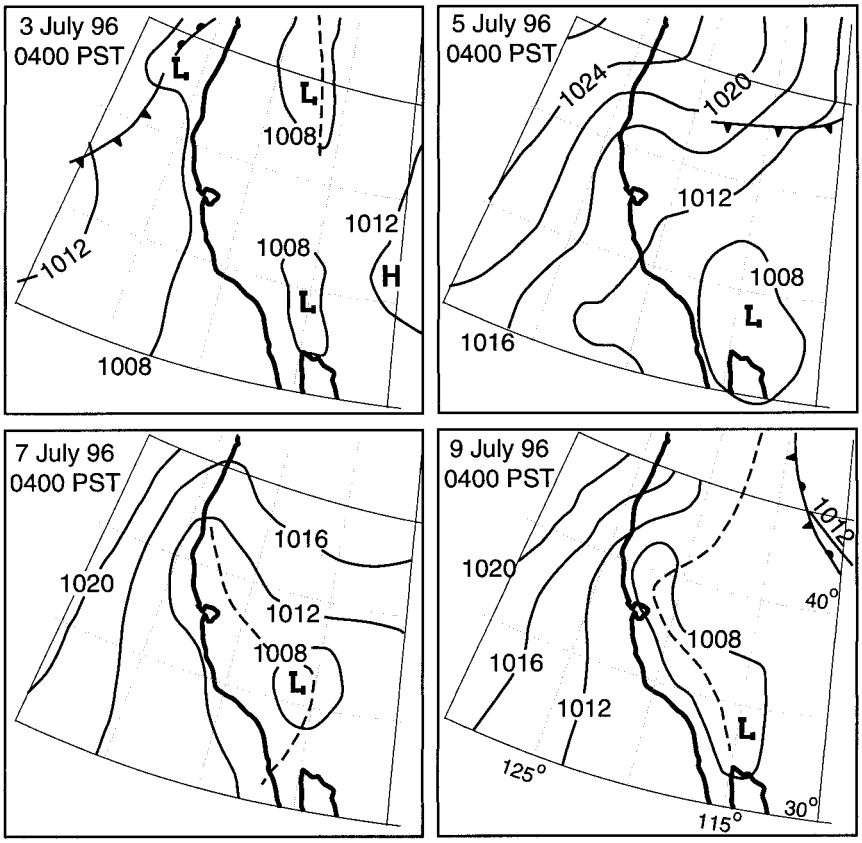

FIG. 8. Sea level pressure analysis (hPa) for Jul 1996. PST is Pacific Standard Time (UTC minus 8 h).

riod for all stations except B11, PARG, and JALM, for which May–July 1995 has been substituted (Fig. 10). In the summer morning, the land is warmer than the sea in the Santa Barbara Channel, with a weak gradient to the east. In the afternoon, all stations are warmer, with the weakest increases over the western mouth and the greatest over the land at the eastern end. Added to the 0600 PST chart are thin dashed lines representing the seasonal averaged SST contours from satellite infrared images. Wind-driven upwelling, associated with the fastest winds, causes the SST minimum in the western mouth (Harms and Winant 1998). The air temperature field is similar to the SST field due to the low heat capacity of the air and the restricted exchange of the marine air with other sources.

A radar profiler operating at Goleta for June and July of 1996 shows three distinct layers and considerable diurnal variation in the structure below 1000 m. The air temperature inversion base is a minimum of 170 m between 2100 and 0100 PST and a maximum of 320 m at 1000 PST (Fig. 11). A similar elevation change trend is followed by the air temperature inversion top with a minimum of 820 m and a maximum of 1070 m. In the air temperature inversion, the strongest winds are offshore at night and the early morning. In the morning, the vertical thermal structure is a marine layer capped by a low air temperature inversion base near 200 m and an air temperature inversion top at 1000 m. In the shallow marine layer, the winds are mostly from the east and weakly onshore. In contrast, the wind in the air temperature inversion is cross shore, from the north. Above the inversion top, winds are from the east. By the middle afternoon, the weakly onshore surface layer is predominantly from the west, while it has reversed to southerly in the air temperature inversion. Above the air temperature inversion top at 1000 m, the winds remain easterly but increase in speed with elevation.

The diurnal phase relationships between Goleta temperature inversion base height and winds are distinct and clearly repeated on most summer days (Fig. 12). In the late morning, the marine layer thickens and the surface winds are westerly while the inversion winds turn southerly. In the early evening, after sunset, the marine layer thins and the surface winds reverse to easterly while the inversion winds are from the north.

The diurnal air temperature inversion base height phase and amplitude at Goleta is similar to that at Gaviota 34 km to the west. During the VOCAR 3-week sounding session in August–September 1993, 2-hourly tethered soundings were made to 1 km. It was found at

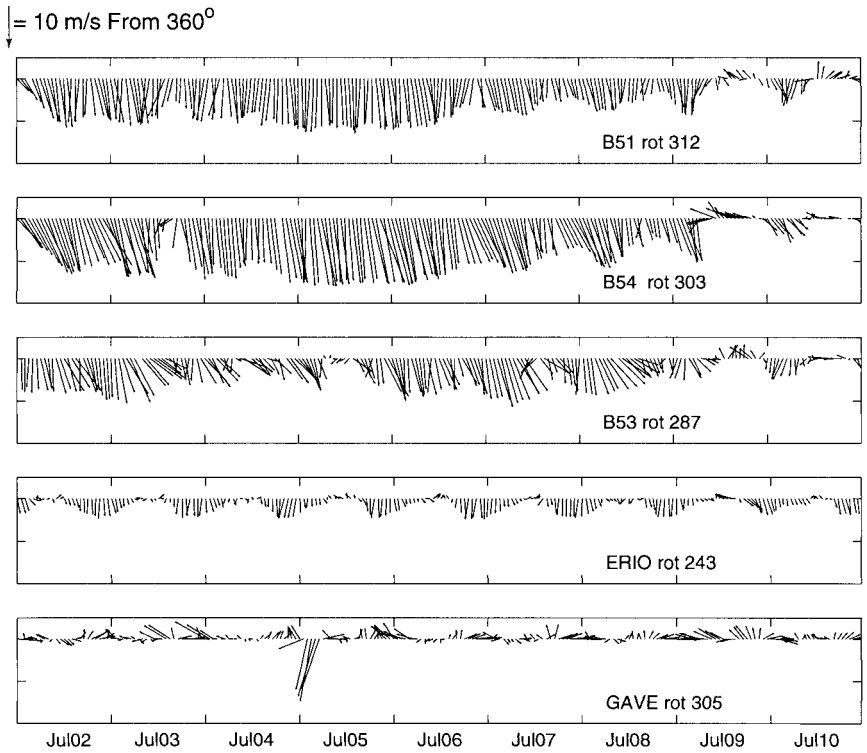

FIG. 9. Surface wind vector time series rotated to the PA for 2–11 Jul 1996 for selected stations.

Gaviota that winds in the lowest 100 km were mostly east–west, while those above could be appreciably cross-shore. Thus, the simple model of cross-coast, diurnally reversing land–sea breeze clearly does not apply here.

e. Larger bight marine-layer structure

We present here a synopsis of the results of the Navy VOCAR sounding program that maintained eight upper-air stations in the Southern California Bight in August and September 1993. In the morning at 0400 PST, the inversion base was lowest in the Santa Barbara Channel and highest in the southern half of the bight (Fig. 13). The strength of the inversion is greater offshore. In the afternoon, at 1600 PST, all base heights are typically about 100 m lower but the lowest is still in the Santa Barbara Channel. The strongest horizontal gradient in the inversion base height is at the western mouth of the Santa Barbara Channel. The greatest inversion strength is to the southwestern portion of the bight while it is weakest in the Santa Barbara Channel.

f. Summer satellite cloud cover

Summer clouds over the ocean in this area are mostly stratus that are restricted to the marine layer. Since the amount of stratus tends to increase with the marine-layer depth (Rosenthal 1972), the amount of cloud cover should be a relative indicator of the marine boundary layer depth. To investigate the cloud structure, the albedo of *GOES-9* visual images were averaged by hour for May–July 1996. The results shown in Fig. 14 are the percent albedo such that 100 would mean a cloud overcast 100% of the time. There is a generally decreasing trend in cloud cover after sunrise that is represented by the hours of 0800, 1200 (not shown) and 1600 PST. At 0800, there is the greatest cloud cover over the water. The marine layer extends across the coastal plains and lower portion of the river valleys, extending the clouds inland to the north of Pt. Arguello, the Oxnard plain, and the coastal plains to the south of Los Angeles. The least clouds are in the lee of Pt. Arguello/Pt. Conception and the western mouth of the Santa Barbara Channel. There is lesser cloud cover over or around all islands, some of which project above the average marine-layer depth. The Channel Islands have a larger area of decreased cloud cover in the lee.

By 1200 PST (not shown), the clouds have greatly decreased in the California Bight and a narrow coastal clear strip to the north. The clear areas in the lees of Pt. Arguello and the Channel Islands have expanded. The largest continuous low cloud area is in the inner coastal zone south of Los Angeles, reflecting the strong subsidence under the returning sea breeze circulation.

At 1600 PST, the low cloud area in the lee of Point

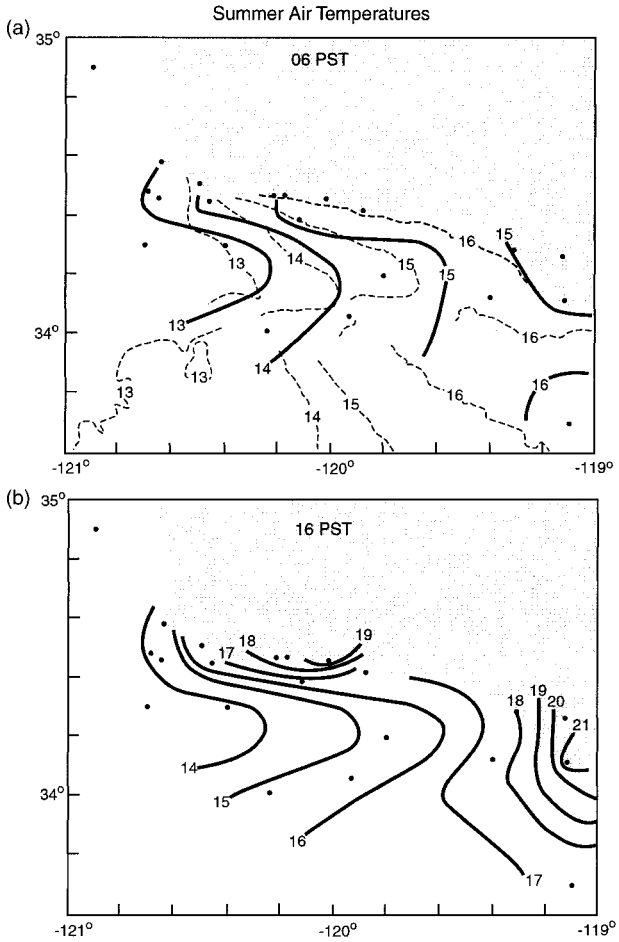

FIG. 10. Summer mean air temperatures (°C) at (a) 0600 PST and (b) 1400 PST. It is coolest in the western mouth. The summer SSTs estimated from satellite infrared images are superimposed on the upper chart as thin dashed lines.

Arguello has extended to all of the Santa Barbara Channel, the Channel Islands lee, and has connected to over water, low cloud areas to the east and southeast. Still, the absolute lowest cloud cover is in the immediate lee of Pt. Arguello and coastline of Santa Barbara Channel and the Channel Islands. Against the trend, cloud cover increased as the marine layer thickened at the coast north of Pt. Arguello. There was also an increase on the northwestern ends of each of the Channel Islands. The summary is that the marine clouds have considerable horizontal structure and a strong diurnal trend over the Southern California Bight. Nevertheless, the marine clouds tend to appear the least in the western mouth of the Santa Barbara Channel throughout the day, and, by inference, the lowest marine layer throughout the day.

The cloud climatology structure in time and space parallels the VOCAR soundings and is consistent with the concept that the marine-layer depth is related to the stratus cloud in the layer. Figure 14 is a proxy map of the relative marine-layer depth structure and its diurnal trend over the Southern California Bight. The result confirms that the lowest marine layer in the area is in the western mouth of the Santa Barbara channel and that there is a higher marine layer on the north side of the Pt. Arguello.

g. Along-coast, diurnal winds

Pressure differences between B54 and B53 are only modestly correlated with B53 winds (Fig. 15). But during some periods, the relationship is weak. The maximum, late afternoon, down channel pressure difference, which is the same for the 4th through the 10th of June 1996, is not correlated with the B54 wind speed maximum that ranges from 13 m s^{-1} on the 4th to 5 m s^{-1} on the 7th and then 15 m s^{-1} on the 10th. Figure 15 also illustrates the comparison between B54 and B53, with the former having periods with high westerly winds with lesser diurnal variation. Station B53 continues to have weak speeds at night, increasing to only about one-half to two-thirds of B54's speed during the afternoon.

All of the winds at stations on the narrow, north coastal plain (zone 3), with the exception of GAVW, have a striking diurnal, alongshore, reversing character. Closer examination was made for phase relationships between the coastal land stations. GAVE and WCAM both had reversing diurnal shifts in the wind on 87% of the summer days, which is typical of the other stations. For GAVE and EMMA, it was found that in the late morning, both stations reverse direction from easterly to westerly and increase in speed until near 1600 PST and EMMA's diurnal maximum. On the other hand, GAVE, some 219 km to the west of EMMA, reverses within an hour to a maximum in the opposite direction. Out of the summer, this near-instant reversing of GAVE while EMMA was still strong westerly occurred on 36% of the days. There was an approximately even amount of these where the reversal occurred simultaneous with EMMA's peak wind as opposed to a little latter while EMMA was still strong westerly.

The wind direction reversal from westerly to easterly in the afternoon/early evening clearly began at the westernmost station (GAVE) and ended with the easternmost station (EMMA) on 39% of the summer days. The approximate timing of these reversals was such that ECAP was an hour later, WCAM was 2 h later, and EMMA was 4 h later.

The wind direction reversal from easterly to westerly in the morning is more uniform in timing without a dominant and distinctive phase trend as in the afternoon. However, in the morning reversals, EMMA reversed to westerly first on 47% of the summer days.

A schematic model is presented that summarizes the dominant diurnal relationship of the north coastal stations (zone 3) winds and the air temperature inversion structure (Fig. 16). In addition, it is assumed that there

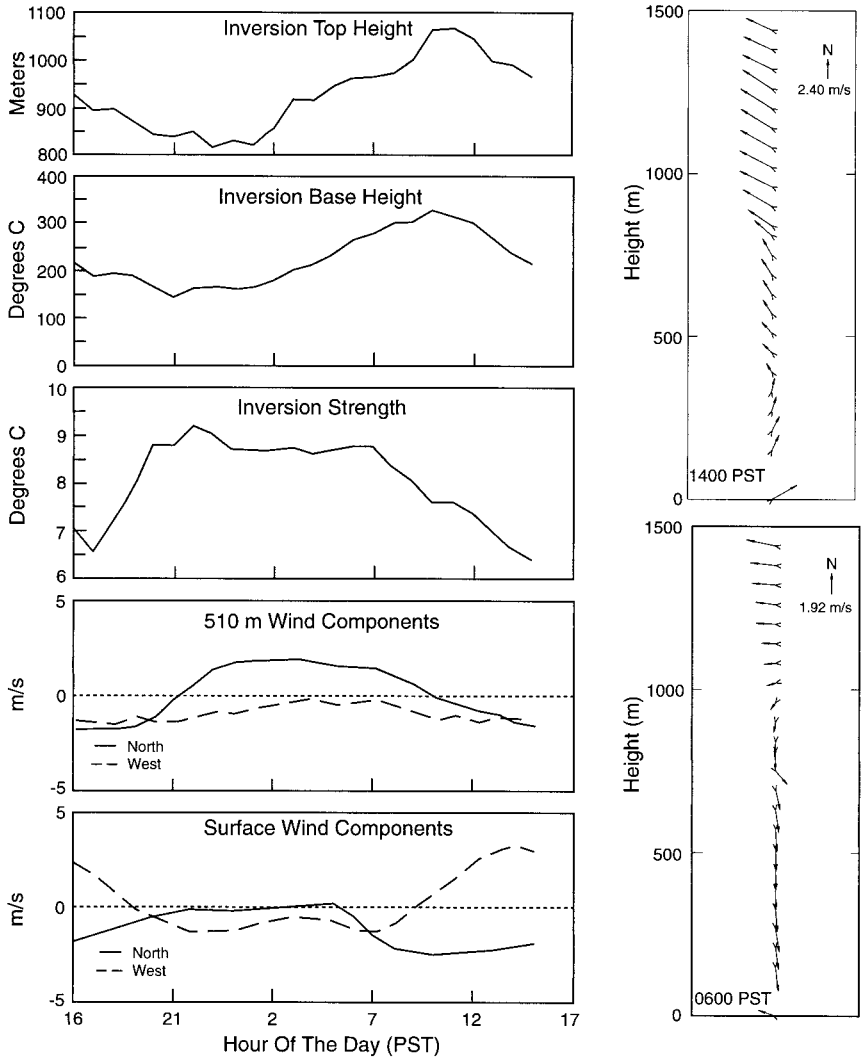

FIG. 11. Selected diurnal trends at the Goleta profiler (GOLE). The air temperature inversion base is a minimum at 2100 PST and a maximum at 1000 PST. Shown on the right is the mean profile for (upper) 1400 PST and (lower) 0600 PST.

is a density-driven, up–mountain slope flow that peaks in the afternoon and a much weaker, down–mountain slope flow that peaks around sunrise (Atkinson 1981), which is consistent with our field experience although not directly measured. At 2100 PST, the inversion is at a minimum elevation, the surface winds are westerly, and the inversion wind is weak. At 0000 PST, the inversion is rising and the inversion base winds are a maximum from the north. By 0600 PST, the inversion base has lifted to the halfway point while the weak downslope flow is a maximum. At 1000 PST, the inversion base is at its maximum elevation, the surface winds are weakly from the south and the inversion winds are weak. By 1400 PST, the inversion base is sinking, the surface winds are peaking in westerly speed while the inversion winds are from the south. Near this time, solar heating maximizes an upslope flow with a subsiding return flow in the inversion over the coast. At 1700 PST, the inversion base has settled to the halfway point and it reaches the minimum elevation at 2100 PST to complete the diurnal cycle.

The general picture is that the inversion base over the coast sinks and the surface winds are from the west during the afternoon. At night, the inversion base lifts and the surface winds are from the east. A cross-coast circulation is set up by the density-driven slope flow that is in the opposite direction of the inversion vertical motion. It is suggested that the inversion base height over the north side of the channel is being forced by the diurnal changes in the overwater expansion fan. This would explain the similar nature of the surface winds at JALM that is around the corner of Pt. Conception

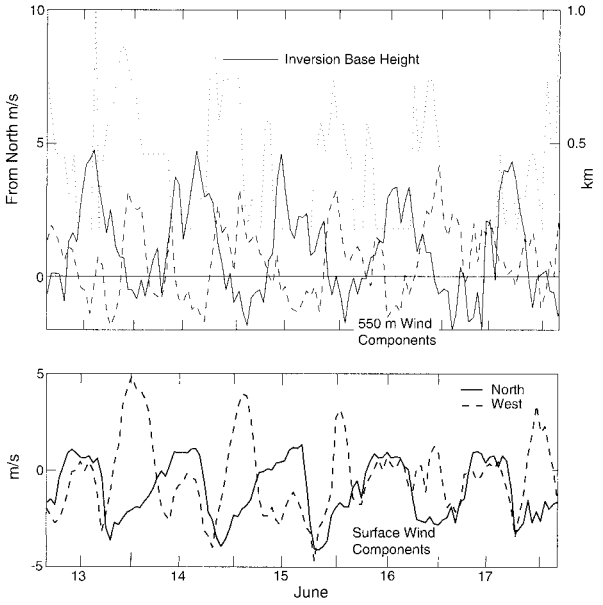

FIG. 12. A short time series showing phase relationship at the Goleta profiler (upper frame). At 550-m elevation, north wind component (solid) is at quadrature to the west component (dashed) in the diurnal period. The inversion base height (dotted) has a distinct, diurnal period too, with a maximum in the late morning, when the 550-m winds are reversing. Surface wind components at Goleta are in the lower frame.

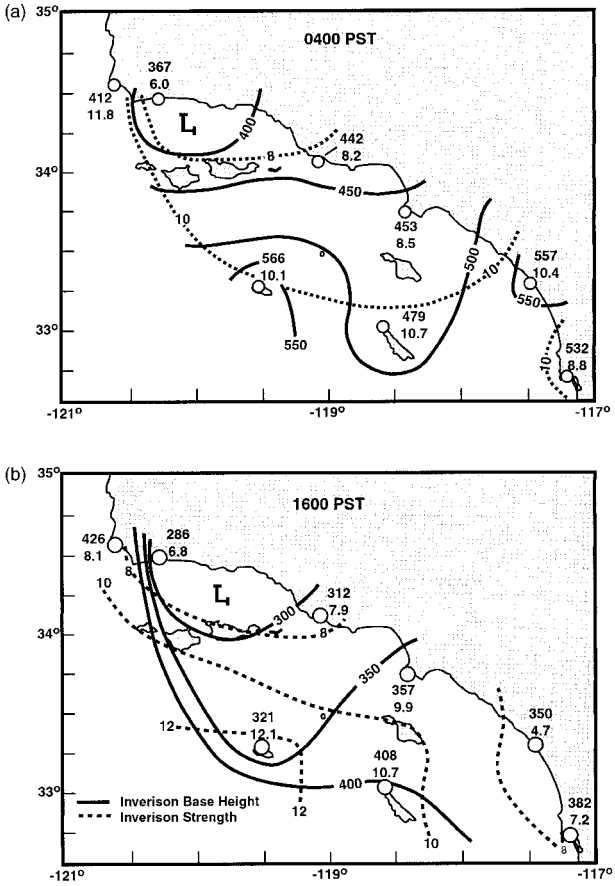

FIG. 13. (a) 0400 PST inversion base height (solid) and strength (dashed). Station's locations are at circles, where the upper plotted number is the air temperature inversion base height in meters and the lower number is the inversion strength in °C. (b) 1600 PST inversion base height and strength. The lowest inversion base height is over the Santa Barbara Channel at both times.

but tucked between the high speed, northerly wind stations of PARG and PCON. However, there is considerable day-to-day variability in the phase of the north coast station reversals.

5. Winter structure and variations

a. Mean fields

Mean winter winds are for the December 1995–February 1996 period for all stations except B11 and JALM. The December 1994–February 1995 observations are used to compute the mean for B11 and JALM as these stations were not available for the 1995/96 season. The winter wind mean and PA for the surface stations are from the northwest at the western mouth and turn to the east in the Santa Barbara Channel (Fig. 17) as during the summer. However, drainage resulting from colder night temperature over the elevated topography flows down the Ventura River valley and causes offshore wind at ERIO, EMMA, and GAIL. There is a mean offshore flow over the north coast stations in contrast to summer. Winter standard deviations are larger than the mean winds and also greater than the summer standard deviations.

Mean winter sea surface pressure gradients are weaker in the winter (Fig. 6). The winter cross-channel gradient is small. The lowest pressures are to the east, as in summer, but the along-channel gradient is half what it is in the summer. This suggests that the vertical thermal structure is uniform across the Santa Barbara Channel in the winter.

b. Correlations and EOFs

Correlations between the overwater wind component along the PA (Fig. 17) are greater in the winter than the summer, which may be due to the longer horizontal scale of winter synoptic events than the summer mesoscale structure. Most of the overwater stations have correlations of 0.7–0.8 or better with neighboring stations. The lowest correlation between a central channel station (B54) and a near-coast station (GAVE) dips to only 0.69. Even the stations away from the Santa Barbara Channel (B11, B25) are correlated with those in it. The poorest correlations are between the land stations at the eastern end of the Santa Barbara Channel.

Winter eigenvectors 1 and 2 are almost the same for the summer (Fig. 17), which confirms the dominant role the local topography plays in surface wind alignment. However, the distribution of eigenvectors (Table 3) is

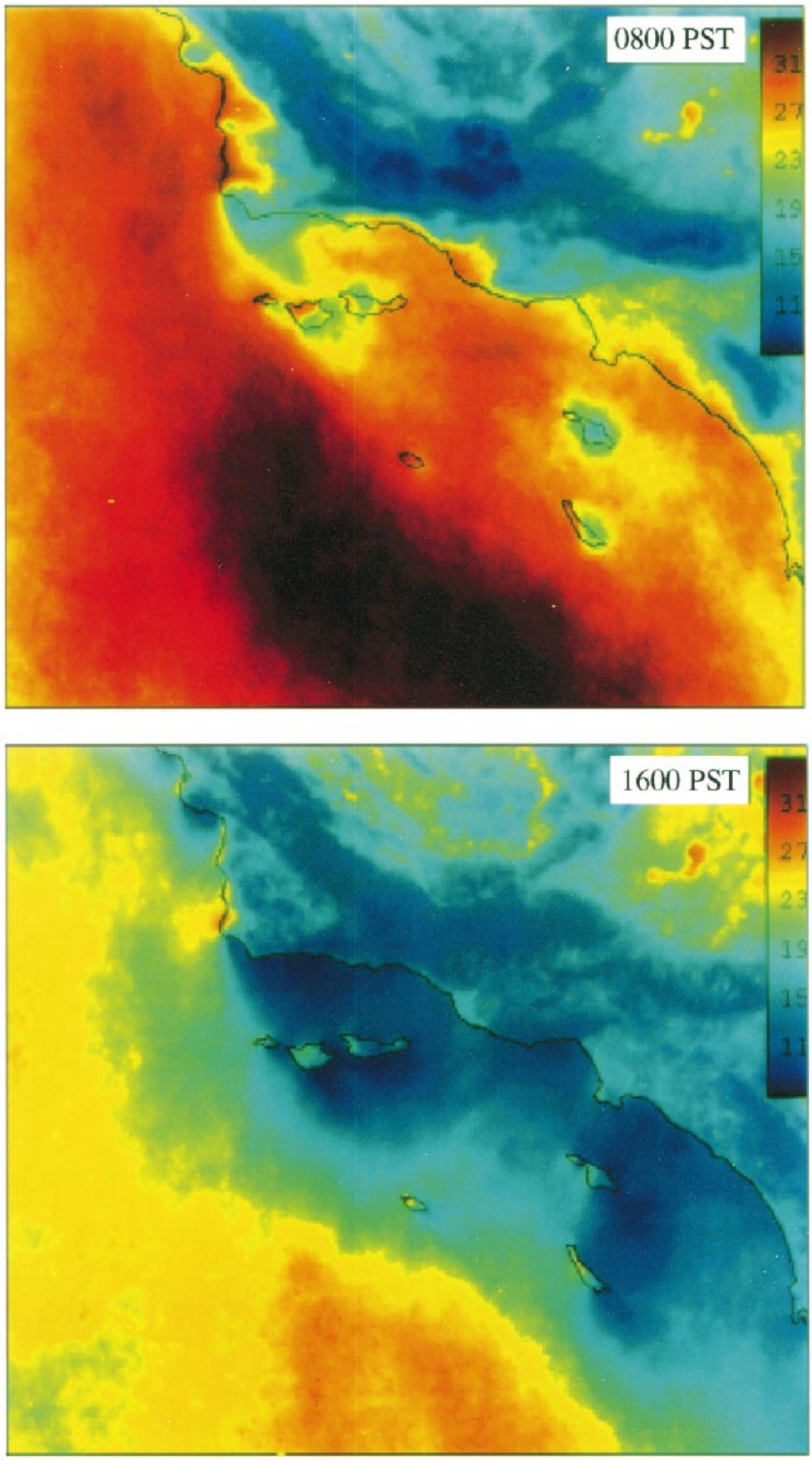

FIG. 14. Average *GOES-9* visual cloud image for 0800 PST (upper) and 1600 PST (lower). The albedo color scale is given in the upper right. The least cloud cover is in the western mouth of the Santa Barbara Channel. At 0800 PST, there is a relatively high cloud cover to the north of Pt. Conception where the marine layer has pushed up against and overrun higher topography. At 1600, clearing continues in the Santa Barbara Channel while the clouds have increased over the edge of land north of Pt. Conception.

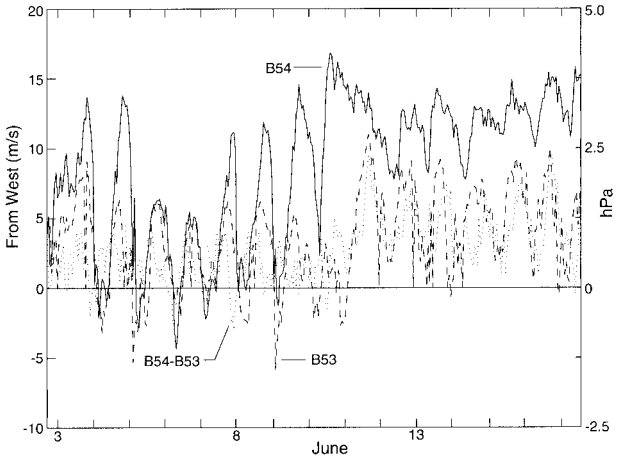

FIG. 15. Summer wind component along PA for B54 (solid) and B53 (dashed) and pressure difference for B54–B53 (dotted). This represents the situation along the central portion of the channel. The pressure difference along the center of the channel is often poorly related to the winds in the western portion and more closely related to those in the eastern portion.

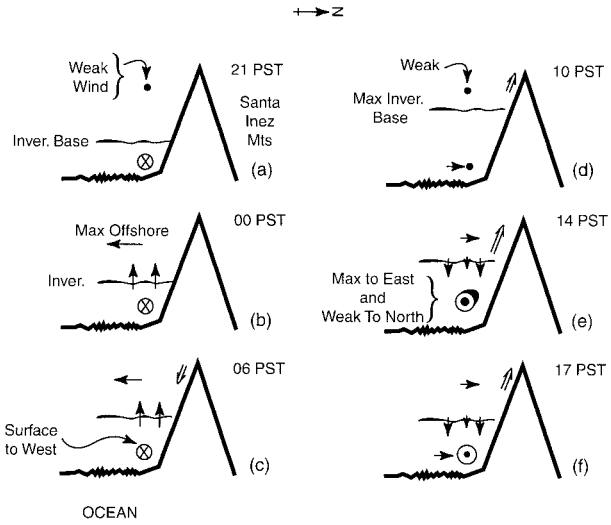

FIG. 16. Westward-looking schematic model of the relation between the north coast station winds and the inversion base height. Mountain up and downslope flow is represented by double arrows.

quite different, reflecting the larger correlation scales. More frequent synoptic-scale variations in the winter cause more persistent peaks in the time series of the winter eigenvector 1 than the summer (Fig. 7). The magnitude and variation of eigenvector 2, which is the diurnal scale, is the same in summer and winter.

c. Synoptic variability

A late-December 1995 case is typical of strong southerly sea level winds followed by a reversal to strong northerly winds. The synoptic situation for strong southerly winds is an approaching front off California and a deep low extending from sea level to above 500 hPa. Sea level and midlevel winds are from the south along central California and the western portion of the Southern California Bight. Later, by 28 December, a ridge oriented northeast–southwest developed across central California from sea level to above 500 hPa and a trough to the east of California. The result was strong winds from the northwest from sea level to the upper atmosphere over the Santa Barbara Channel.

Strong southerly winds at the western Santa Barbara Channel surface stations extended from 22 to 26 December with the winds increasing in strength from the Islands to B51 (Fig. 18). Winds were slower and from the east in the eastern portion of the channel. North coastal stations varied between periods of southerly and alongshore winds.

The winds reversed abruptly around midnight on 26–27 December to be strong from the north-northwest of the western channel until 1 January. Winds increased from B51 to maximum at B54 then mildly decreased at the islands. The north coast stations such as GAVE experienced persistent offshore winds but at speeds less than at the islands. Finally, winds were weak and variable in direction at the eastern coastal station ERIO.

d. Diurnal variability

Winter diurnal trends over the water (not shown) have a phase relation similar to diurnal trends during the summer. However, the diurnal range is less and the overwater stations' values are reduced at all hours. The exception is the Oxnard station at ERIO, which has a stronger and longer duration easterly component lasting from 1900 to 0900 during the winter.

Winter air temperatures shown in Fig. 19 are for the December 1995–February 1996 period for all stations except B11, PARG, and JALM, for which December 1994–February 1995 has been substituted. In the winter morning, there is a weak air temperature maximum over the center of the channel while the strongest minimum is over the Oxnard Plain on the eastern end. By the afternoon, stronger diurnal warming has reversed the situation so that the warmest temperatures are over land. Somewhat similar to the summer, there are along- and cross-channel gradients with the coldest air at the western mouth of the channel. However, satellite-derived SSTs (thin dashed lines in Fig. 19) are nearly uniform over the Santa Barbara Channel.

6. Eddies

Two eddies have been found in the sea level wind field over the Santa Barbara Channel based upon September–October 1980 observations collected for an air pollution study that are presented in Fig. 20 (Smith et al. 1983; Dabberdt and Viezee 1987; Douglas and Kessler 1991; Hanna et al. 1991). We find that these are typical of neither the summer nor the winter, although

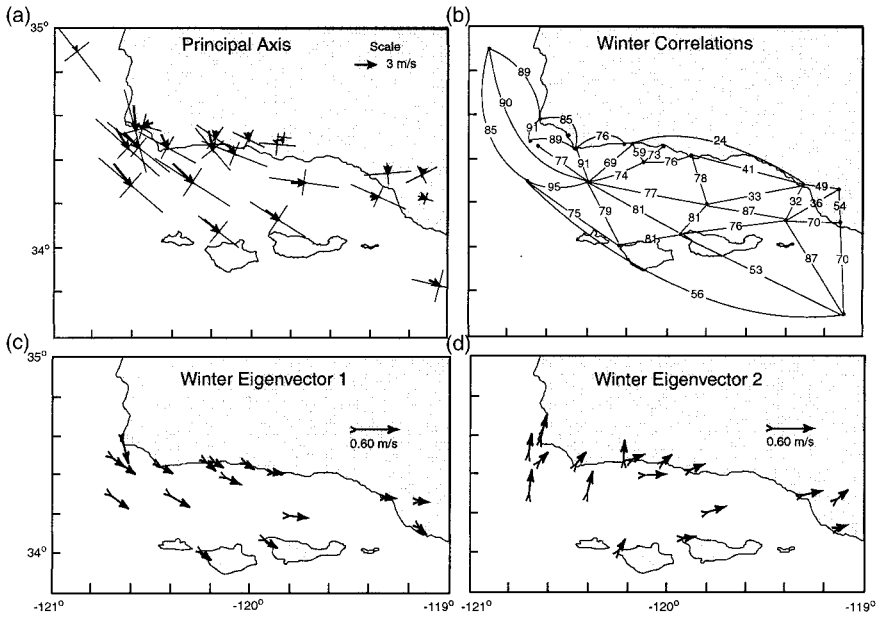

FIG. 17. (a) Winter mean surface wind speed and principle axis (PA). See Fig. 4 for explanation. (b) Winter wind correlations along station PAs. (c) and (d) First and second empirical orthogonal functions for the winter (lower panels).

this probably reflects the different time periods of the studies and the focusing on a particular light wind situation that is associated with late summer air pollution events.

The first is in regards to an evening, midchannel, cyclic eddy (Smith et al. 1983) (Fig. 20a). The midchannel buoys (B54, B53) and platform GAIL showed that the marine air moves zonally along the center of

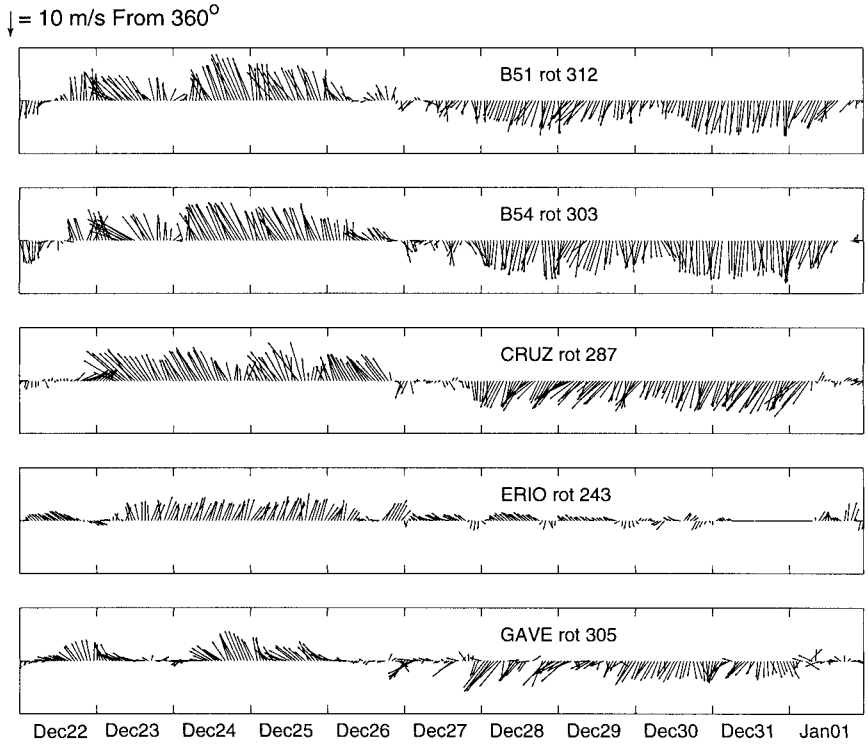

FIG. 18. Surface station wind vector series rotated to the PA for 22 Dec 1995–2 Jan 1996.

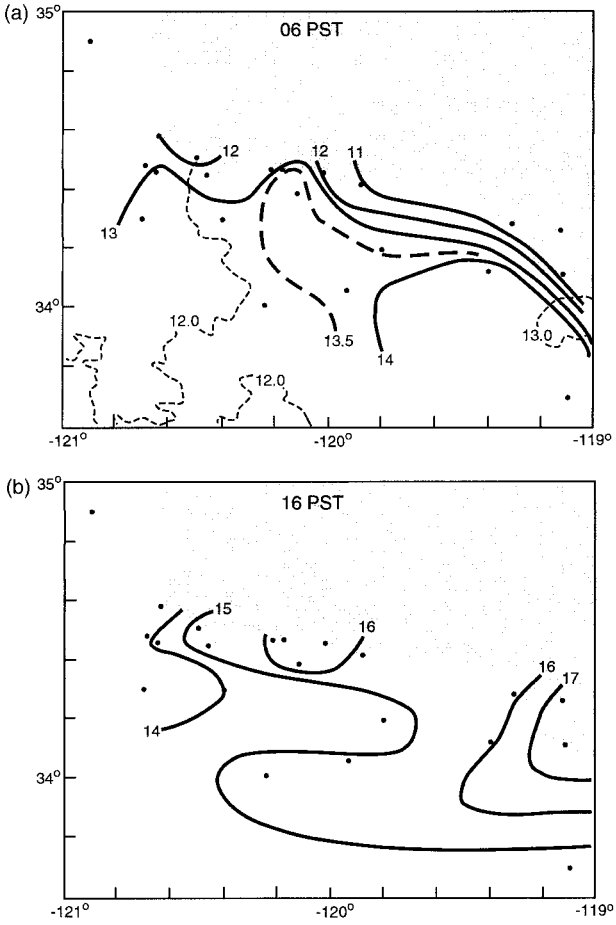

FIG. 19. Winter mean air temperatures (°C) at (a) 0600 PST and (b) 1400 PST. The winter SSTs estimated from satellite infrared images are superimposed on the upper chart as thin dashed lines.

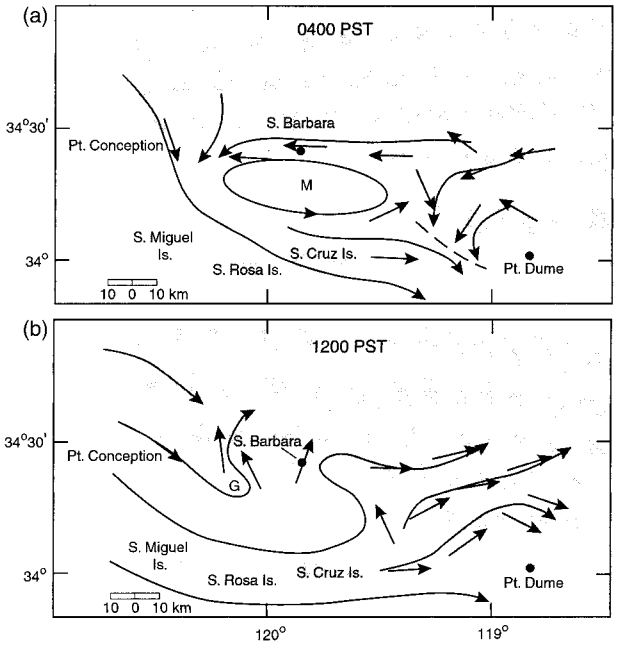

FIG. 20. Streamlines of most frequent September wind directions from Smith et al. (1983) and Dabberdt and Viezee (1987). Arrows are measured winds. Here M marks midchannel eddy in (a) and G denotes Gaviota eddy in (b).

the channel and from the west. The majority of this air mass moves from the northwest past GAIL, whereas the air pollution analysis had winds from the southeast at GAIL. Our analysis suggests that if the winds at B54 are strong, there is no midchannel eddy, which occurs most of the time.

In addition, our analysis does not support a summer, daytime Gaviota eddy in the lee of Pt. Conception (Fig. 20b), although this may be partly semantics. Our analysis suggests that the dominant winds between Gaviota (GAVE) to Ventura (EMMA) are coast-parallel and diurnally reversing. The along-coast afternoon winds are part of the zonal, westerly flow, unlike the cross-shore, coastal winds found during the air pollution studies. Easterly, evening winds over the coastal stations are consistent with the earlier studies, but there is a very narrow transition zone into the westerly and stronger flow over most of the channel. We would classify this as a shear zone, rather than an eddy owing to the difference in speeds and the narrowness of the transition between the two flow directions. We also find a different phase relationship among the coastal stations, such that the western coastal stations will reverse before the eastern coastal station (EMMA). On most of the days, especially under lighter winds, the finer aspects of the timing of the direction changes at the coastal stations are erratic, defying simple classification.

7. Dynamical interpretation

a. A model

The presence of a marine layer between the ocean and the free atmosphere with distinct air mass properties allows for the existence of gravity waves, which can propagate along the inversion. The existence of these waves has been documented in a number of studies (Atkinson 1981), and different models for the wave propagation have been proposed (Gossard and Hooke 1975). The possibility for gravity waves to exist and propagate at some speed also has implications for steady flows, and hydraulic flow theory provides the context for describing the development of such flow (Ippen 1951). The behavior of a steady hydraulic flow depends critically on the Froude number, the ratio of the flow speed, and the speed of gravity waves propagating on the inversion. If the Froude number is less than unity, the presence of obstacles in the flow can extend upstream of the obstacle and the flow is subcritical. If the Froude number is greater than one, no flow adjustment can occur upstream and the flow is supercritical (Samelson 1992).

Observations of the marine layer off the California

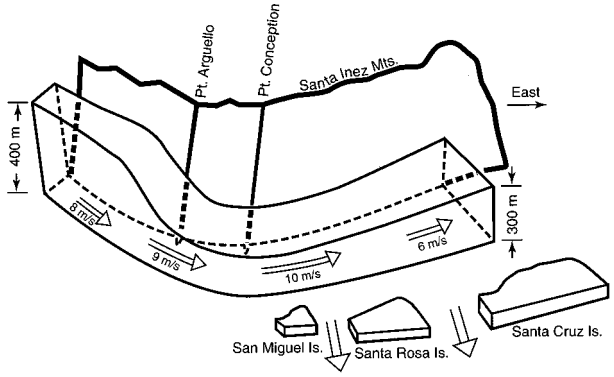

FIG. 21. Schematic model of the marine-layer structure turning into the Santa Barbara Channel. The marine air thins, expands, and accelerates as it turns the corner into the Santa Barbara Channel, causing the fastest winds to be at the western mouth.

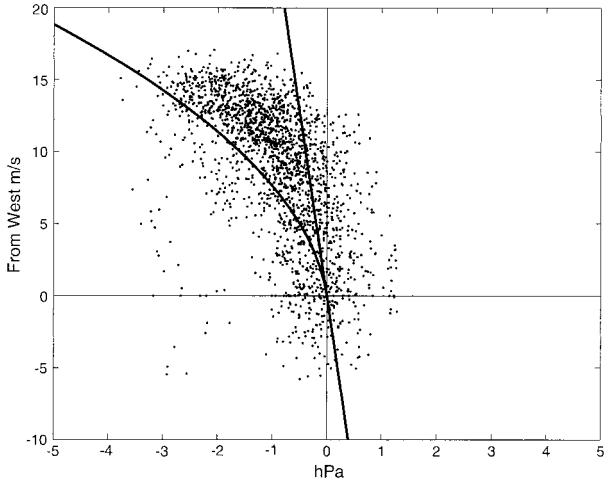

FIG. 22. Scatterplot of hourly B54 wind as a function of the HOND–ROSA pressure difference. The straight line is the expectation if there were a purely geostrophic balance. The quadratic line is the expectation if there were a strong supercritical expansion.

coast (Dorman 1985b; Winant et al. 1988; Samelson and Lentz 1994) suggest that at any time the flow can shift between sub- and supercritical conditions as a function of position, a condition described as transcritical (Rogerson 1999).

The conditions in the western mouth (zone 1) are very much like a supercritical or transcritical expansion fan in the lee of a corner. A schematic model in Fig. 21 summarizes the details. Under strong, supercritical flow to the south or southeast, the near–sea level air accelerates from around the area between Pt. Arguello and Pt. Conception to the speed maximum, near B54. At the same time, the atmospheric marine layer expands and thins to a minimum height and the sea level pressure decreases. The inversion also tilts downward to the north across the channel, making the lowest inversion base along the north coast as shown in Fig. 13. As marine air continues eastward toward B53, it slows and the vertical dimension increases. Some of the air mass entering the western mouth exits at supercritical speeds via the gaps between the channel islands. The low air temperature inversion base over the north coast intersects the topography, capping the marine air and limits vertical exchange. With no outlet to the north, the coastal winds run parallel to the coast, even during the height of diurnal heating cycle.

The descriptive details provided in the preceding sections support this model. The surface winds accelerate into the mouth to a maximum speed, then decrease toward the eastern portion of the channel. Fixed soundings show that the Santa Barbara Channel has the lowest inversion base in the Southern California Bight. Satellite cloud averages have structures that are consistent with deeper marine layers outside the western mouth, lowering into the western Santa Barbara Channel. Cloud analysis also confirms lower clouds and supercritical expansion in the lee of the gaps between the Channel Islands.

The lack of sounding data over water and north of Pt. Conception prevents a clear identification as to the Froude number of the inbound marine layer. However, the relatively low velocities and deeper marine layer at B11 suggests that both the inbound flow and the outbound velocities in the eastern half of the Santa Barbara Channel are subcritical. Only the western mouth of the channel is supercritical. This pattern conforms to the transcritical flow in the lee as described by Rogerson (1999).

b. Supercritical flow and surface stations

Whether or not the Froude number is greater than one and the flow is supercritical can be estimated from the sea level wind and pressure observations at the western mouth. The cross-channel pressure gradient can be computed from SROS minus HOND pressures, which are separated by 40 km. The along-PA component at B54 was used for the surface wind. A scatterplot of the pressure difference versus wind speed for May–July 1996 is presented in Fig. 22. If the momentum balance is geostrophic, the pressure difference may be related to the wind speed by the following geostrophic relationship,

$$dP = \rho f V\, dx,$$

where ρ is the density, f is the Coriolis parameter, V is the wind speed perpendicular to the two stations, and dx is the pressure station separation. As noted in Winant et al. (1988), using a modification of Bernoulli's equation we can compute the maximum pressure difference expected if the flow is supercritical and frictionless, and if the inbound Froude number is one and the downstream Froude number is infinite. Across the expansion fan, the speed should be related to the pressure by the quadratic,

$$dP = \rho V(f\, dx - V),$$

which represents the sum of the geostrophic difference and the maximum difference expected for a supercritical expansion. The density is assumed to be 1.2 kg m^{-3}, the Coriolis parameter is 8.2×10^{-5} s^{-1}, and the distance between the pressure stations is 40 km. Most of the intermediate and higher speeds fit between the quadratic and the line that is also plotted in Fig. 22. A similar result was found in the lee of Pt. Arena by Winant et al. (1988) and supports the existence of a transcritical expansion fan.

c. Summer versus winter

It is useful to compare the summer and winter seasons for the role of supercritical flow in modifying characteristics. The summer sea level pressure gradient is both stronger and asymmetrical across the channel (lower on the north side). A major contributor to the asymmetry is the thinner marine layer on the north side. For every 100 m below the marine layer, the surface pressure would be reduced by the order of 0.5 hPa (Dorman 1985a). That the marine layer is low in the Santa Barbara Channel is confirmed by the VOCAR and other limited sounding programs and supported by the satellite cloud climatology.

Summer sea level air temperatures are a minimum in the western mouth of the Santa Barbara Channel and are not apparent in the winter mornings. The difference is the summer's stronger westerly winds in the western mouth force upwelling and attendant SST minimums with a similar pattern. In the winter, the SST gradient is almost flat.

Summer mean winds over the western mouth of the Santa Barbara channel are faster than in the winter, although the standard deviation of the winds is similar in both seasons. Winter experiences strong winds either from a northerly or a southerly direction. On the other hand, only summer experiences strong winds from a northerly direction.

8. Conclusions

Weather patterns in the Santa Barbara Channel vary markedly depending on the season. In late spring, summer, and fall, the weather results from the interaction between two persistent large-scale systems, the North Pacific anticyclone and the thermal low located over the southwestern United States. Partly because of the subsidence associated with the anticyclone, a well-defined marine atmospheric boundary layer (MABL) with properties distinct from the free atmosphere above is a conspicuous feature during the summer. The wind has different characteristics in each of three zones. Maximum winds occur in the area extending south and east from Pt. Conception, where they initially increase as they turn to follow the coast, then decrease farther east. Winds are generally weaker, sometimes reversing to easterly at night, in a narrow band along the mainland coast. They are also weak in the easternmost part of the channel, offshore from the Oxnard plain. Air temperature at the surface follows the SST closely and varies significantly with location. Sea level pressure gradients are correspondingly large. The height of the marine layer varies generally between 300 m in the late afternoon and 350 m in the late morning.

In winter, synoptic conditions are driven by traveling cyclones, sometimes accompanied by fronts. These are usually preceded by strong southeast winds and followed by strong northwest winds. Atmospheric parameters are distributed more uniformly than in summer and diurnal variations are greatly reduced. Sea level air temperature and pressure are more uniform spatially than in the summer.

Spatial variations in the observed fields in the summer are consistent with a hydraulic model of the MABL involving a transcritical expansion fan. The summertime situation is governed by a coupled interaction between the atmosphere and the underlying water. The ocean influences the density of the MABL to the extent that it behaves distinctly from the free atmosphere above, resulting in strong winds polarized in the direction parallel to the coast. In turn these winds provoke an upwelling response in the coastal ocean, which in part determines the surface properties of the water as is noted in Harms and Winant (1998).

Acknowledgments. We are especially grateful to the Santa Barbara Air Pollution Control District, the Ventura Air Pollution Control District, and Point Mugu NAS for sharing data that was essential for this analysis. Lee Eddington supplied data from the navy-sponsored VOCAR program. Dick Lind was crucial in capturing and transferring upper-air data. David Browne of MMS helped obtain access to platforms and was an essential link to the core funding. This paper was funded by the Mineral Management Service and the Office of Naval Research.

REFERENCES

Atkinson, B. W., 1981: *Meso-Scale Atmospheric Circulations.* Academic Press, 495 pp.

Baynton, H. W., J. M. Bidwell, and D. W. Beran, 1965: The association of the low-level inversions with surface wind and temperature at Point Arguello. *J. Appl. Meteor.,* **4,** 509–516.

Bosart, L. F., 1983: Analysis of a California Catalina eddy event. *Mon. Wea. Rev.,* **111,** 1619–1633.

Brink, K. H., and R. D. Muench, 1986: Circulation in the Point Conception–Santa Barbara Channel region. *J. Geophys. Res.,* **91,** 877–895.

Caldwell, P. C., D. W. Suart, and K. H. Brink, 1986: Mesoscale wind variability near Point Conception, California, during spring 1983. *J. Climate Appl. Meteor.,* **25,** 1241–1254.

Clark, J. H. E., and S. R. Dembek, 1991: The Catalina eddy event of July 1987: A coastally trapped mesoscale response to synoptic forcing. *Mon. Wea. Rev.,* **119,** 1714–1735.

Dabberdt, W. F., and W. Viezee, 1987: South Central Coast Cooperative Aerometric Monitoring Program (SCCCAMP). *Bull. Amer. Meteor. Soc.,* **68,** 1098–1110.

Dana, R. H., 1841: *Two Years Before the Mast: A Personal Narrative of Life at Sea.* Harper, 483 pp.

DeMarrias, G. A., G. C. Holzworth, and C. R. Hosler, 1965: Meteorological summaries pertinent of atmospheric transport and dispersion over southern California. U.S. Weather Bureau Tech. Paper 54, 86 pp. [Available from Superintendent of Documents, U.S. Government Printing Office, Washington, DC 20401.]

Dorman, C. E., 1982: Winds between San Diego and San Clemente Island. *J. Geophys. Res.,* **87,** 936–946.

——, 1985a: Evidence of Kelvin waves in California's marine layer and related eddy generation. *Mon. Wea. Rev.*, **113,** 827–839.

——, 1985b: Hydraulic control of the northern California marine layer. *Eos, Trans. Amer. Geophys. Union,* **66,** 914.

——, 1987: Possible role of gravity currents in northern California's coastal summer wind reversals. *J. Geophys. Res.*, **92,** 1497–1506.

——, and C. D. Winant, 1995: Buoy observations of the atmosphere along the west coast of the United States, 1981–1990. *J. Geophys. Res.*, **100,** 16 029–16 044.

Douglas, S. G., and R. C Kessler, 1991: Analysis of mesoscale airflow patterns in the south-central coast air basin during the SCCCAMP 1985 intensive measurement periods. *J. Appl. Meteor.,* **30,** 607–631.

Eddington, L. W., 1985: A numerical simulation of a topographically forced wind maximum in a well-mixed marine layer. OPUS Tech. Rep. 16, FSU-MET-OPUS-85-1, 61 pp. [Available from Dept. of Meteorology, The Florida State University, Tallahassee, FL 32306.]

——, J. J. O'Brien, and D. W. Stuart, 1992: Numberical simulation of topographically forced mesoscale variability in a well-mixed marine layer. *Mon. Wea. Rev.,* **120,** 2881–2896.

Edinger, J. G., 1959: Changes in the depth of the marine layer over the Los Angeles basin. *J. Atmos. Sci.,* **16,** 219–226.

——, 1963: Modification of the marine layer over coastal southern California. *J. Appl. Meteor.,* **2,** 706–712.

——, and M. G. Wurtele, 1972: Interpretation of some phenomena observed in southern California stratus. *Mon. Wea. Rev.,* **100,** 389–398.

Fisk, C., 1994: Mesoscale hourly variation in surface meteorological parameters during the intensive operation of Vocar 22 August 1993–4 September 1993. Geophysics Division Tech. Note No. 187, 43 pp. [Available from Naval Air Warfare Center, Weapons Division, Point Mugu, CA 93042-5001.]

Gossard, E. E., and W. H. Hooke, 1975: *Waves in the Atmosphere, Atmospheric Infrasound and Gravity Waves—Their Generation and Propagation.* Elsevier, 456 pp.

Halliwell, G. R., and J. S. Allen, 1987: The large-scale coastal wind field along the west coast of North America. *J. Geophys. Res.*, **92,** 1497–1506.

Hamilton, G. D., 1980: NOAA Data Buoy Office programs. *Bull. Amer. Meteor. Soc.,* **61,** 1012–1017.

Hanna, S. R., D. G Strimaitus, J. S. Scire, G. E. Moore, and R. C. Kessler, 1991: Overview of results of analysis of data from the South-Central Coast Cooperative Aerometric Monitoring Program (SCCCAMP 1985). *J. Appl. Meteor.,* **30,** 511–533.

Harms, S., and C. D. Winant, 1998: Characteristic patterns of the circulation in the Santa Barbara Channel. *J. Geophys. Res.,* **103,** 3041–3065.

Ippen, A. T., 1951: Mechanics of supercritical flow. *Trans. Amer. Soc. Civ. Eng.,* **116,** 268–295.

Kessler, R. C., and S. G. Douglas, 1991: Numerical study of mesoscale eddy development over the Santa Barbara Channel. *J. Appl. Meteor.,* **30,** 633–651.

Large, W. G., and S. Pond, 1981: Open ocean momentum flux measurements in moderate to strong winds. *J. Phys. Oceanogr.,* **11,** 324–481.

Lorenz, E. N., 1956: Empirical orthogonal functions and statistical weather prediction. MIT Sci. Rep. 1, 49 pp. [Available from Stat. Forecasting Project, Department of Meteorology, Massachusetts Institute of Technology, Cambridge, MA 02139.]

Mass, C. F., and M. D. Albright, 1987: Coastal southerlies and alongshore surges of the west coast of North America: Evidence of mesoscale topographically trapped response to synoptic forcing. *Mon. Wea. Rev.*, **115,** 1707–1738.

——, and ——, 1989: Origin of the Catalina eddy. *Mon. Wea. Rev.*, **117,** 2406–2436.

Neiburger, M., D. S. Johnson, and C. W. Chien, 1961: Studies of the structure of the atmosphere over the eastern Pacific Ocean in the summer. *The Inversion over the Eastern North Pacific Ocean,* University of California Press, 1–94.

Nelson, C. S., 1977: Wind stress and wind stress curl over the California Current. NOAA Tech. Rep. NMFS SSRF-714, 87 pp. [Available from National Oceanic and Atmospheric Administration, Monterey, CA 93940.]

——, and D. M. Husby, 1983: Climatology of surface heat fluxes over the California current region. NOAA Tech. Rep. NMFS SSRF-763, 155 pp.

Paulus, R. A., 1995: An overview of an intensive observational period on variability of coastal atmospheric refractivity. *Proc. AGARD/NATO Conf. on Propagation Assessment in Coastal Environments,* Bremerhaven, Germany, NATO, 1–6.

Ralph, F. M., L. Armi, J. M. Bane, C. E. Dorman, W. D. Neff, P. J. Neiman, W. Nuss, and P. O. G. Persson, 1998: Observations and analysis of the 10–11 June 1994 coastally trapped disturbance. *Mon. Wea. Rev.*, **126,** 2435–2465.

Reason, C. J. C., and D. G. Steyn, 1992: The dynamics of coastally trapped mesoscale ridges in the lower atmosphere. *J. Atmos. Sci.,* **49,** 1677–1692.

Rogerson, A. M., 1999: Transcritical flows in the coastal marine atmospheric boundary layer. *J. Atmos. Sci.,* **56,** 2761–2779.

Rosenthal, J., 1968: A Catalina eddy. *Mon. Wea. Rev.*, **96,** 742–743.

——, 1972: Point Mugu Forecasters Handbook. Pacific Missile Range, Tech. Publ. PMR-TP-72-1, 324 pp. [Available from Geophysics Branch, Pacific Missile Range, Pt. Mugu, CA 93042-5001.]

Ryan, G., 1996: Downslope winds of Santa Barbara, California. NOAA Tech. Memo. NWS WR-240, 44 pp. [Available from National Technical Information Service, U.S. Department of Commerce, 5285 Port Royal Rd., Springfield, VA 22161.]

Samelson, R. M., 1992: Supercritical marine-layer flow along an smoothly varying coastline. *J. Atmos. Sci.,* **49,** 1571–1584.

——, and S. J. Lentz, 1994: The horizontal momentum balance in the marine atmospheric boundary layer during CODE-2. *J. Atmos. Sci.,* **51,** 3745–3757.

Smith, T. B., W. D. Saunders, and F. H. Shair, 1983: Analysis of Santa Barbara oxidant study. Final Report to California Air Resources Board, Agreement A2-086-32, 236 pp. [Available from Meteorology Research, Inc., Altadena, CA 91001.]

Sommers, W. T., 1978: LFM forecast variables related to Santa Ana wind occurrences. *Mon. Wea. Rev.,* **106,** 1307–1316.

Thornthwaite, C. W., W. J. Superior, and R. T. Field, 1965: Disturbance of airflow around Argus Island Tower near Bermuda. *J. Geophys. Res.*, **70,** 6047–6052.

Wakimoto, R. M., 1987: The Catalina eddy and its effects on pollution over southern California. *Mon. Wea. Rev.*, **115,** 837–855.

Winant, C. D., C. E. Dorman, C. A. Friehe, and R. C. Beardsley, 1988: The marine layer off northern California: An example of supercritical channel flow. *J. Atmos. Sci,* **45,** 3588–3605.